

# Combined soft nanotechnology methods — as versatile tools for designing templated nanostructures to obtain optically active materials

NICOLETA-LILIANA OLTEANU<sup>1</sup>, ADINA ROXANA PETCU<sup>1</sup>, COSMINA ANDREEA LAZAR<sup>1</sup>, AURELIA MEGHEA<sup>1</sup>, ELENA ADINA ROGOZEA<sup>1,\*</sup> AND MARIA MIHALY<sup>2,\*</sup>

<sup>1</sup>*Research Centre for Environmental Protection and Eco-friendly Technologies, University Politehnica of Bucharest, Polizu 1, 011061, Bucharest, Romania*

<sup>2</sup>*Faculty of Applied Chemistry and Materials Science, University Politehnica of Bucharest, Polizu 1, 011061, Bucharest, Romania*

*Received: October 20, 2015. Accepted: November 2, 2015*

Since the discovery of microemulsions, the increasing interest both in basic research and in different industrial fields became more significant due to their unique properties, namely, large interfacial area, ultralow interfacial tension, thermodynamic stability and the ability to solubilize otherwise immiscible liquids. In recent years, nanoparticles have gained an increasing interest because of their unique size dependent properties (electrical, magnetic, mechanical, optical and chemical) which largely differ from those of corresponding bulk materials. As it is already known, by precise control of microemulsion composition and morphology, the special properties of the nanoparticles can be enhanced by their incorporation and/or coating with different matrices. Recently, the microemulsion assisted sol-gel procedure used to control the size, shape and distribution of nanoparticles, was applied as a versatile tool to prepare inorganic and hybrid silica based materials with results in technological application, such as: electrochemical, solar collectors, photocatalysis wastewater treatment and NLO materials. This paper aims to offer a vivid look on the use of microemulsions assisted sol-gel procedure for synthesizing and controlling the size and morphology of the nanoparticles and in the same time some recent works carried out in the synthesis and application of organic and inorganic silica based materials by this method are reviewed.

*Keywords: Nanoparticles synthesis, Microemulsions, NLO materials*

---

\*Corresponding authors: adinarogozea@gmail.com, maria.mihaly@upb.ro

## 1. INTRODUCTION

Nanosized materials such as *quantum dots*, nanoparticles, nanowires and nanotubes or nanostructured materials have attracted a special attention due to their interesting properties that cannot be found in the case of macroscopic materials [1]. Nanomaterials unique properties determined by their quantum size effect lead to the narrowing of the structure bands by forming distinct quantum levels. These materials are among the most promising sources of scientific and technological research, since one can tune their optical, magnetic, electrical, catalytic, and drug transporter properties [2, 3]. In addition, their physical properties such as mechanical resistance, thermal stability and chemical passivity are well improved. Nanoparticles, more and more applied in various fields in science, industry and environment, resulted in a straightforward need for new synthesis and characterization techniques of these types of materials.

Both inorganic and organic nanoparticles have been synthesized by a variety of physical and chemical methods like chemical reduction [4-6], thermal [7], irradiation [8, 9] or methods using laser ablation [10]. Among these methods microemulsification is one of the most efficient preparation methods, which allows the control of nanoparticle properties such as size, geometry, morphology, homogeneity and surface area. Furthermore, the development of a new recent method, namely, the microemulsion assisted sol-gel process [11-15] has resulted in silica based materials with special properties. The potential advantages of this strategy for silica based materials preparation are: i) the inorganic and organic nanoparticles are obtained directly in the microemulsion; ii) the nanoparticles size and shape can be controlled to a great extent therefore a narrow particles size distribution can be obtained; iii) the nanoparticles entrapment is based on the formation of the silica network around them, acting as crystallization nuclei within the microemulsion colloidal aggregates.

This article reviews the recent utilization of microemulsions assisted sol-gel procedure for the synthesis of metallic, metallic oxide and organic nanoparticles and summarizes the works carried out in the synthesis and application of organic and inorganic silica based materials by this method.

## 2. GENERAL METHODS FOR NANOPARTICLES SYNTHESIS

The main methods for nanoparticles synthesis are chemical, mechanical, *in situ* and in gaseous phase.

### 2.1. Chemical methods

Chemical methods for nanoparticles synthesis encompass colloidal chemistry, hydrothermal process, sol-gel and other precipitation reactions [4-6, 16].

The precipitates obtained by controlling the solutions of different ions mixture in well-established ratios, the temperature and pressure, and insoluble compounds were collected by filtration and dried in order to obtain final nanoparticles powders. Both organic and inorganic materials are the result of these methods by simple and low cost equipment and in significant amounts. Other important advantages of this synthesis route are the strict control of their size and the final materials have high monodispersity. These methods have also some limitations like the small yields of the sol-gel processes. A new approach that can eliminate these drawbacks was the use of micellar microreactors where are synthesized well-dispersed nanoparticles.

## **2.2. Mechanical methods**

Mechanical processes encompass milling and mechanical alloying and uses physical techniques of spraying in increasingly finer powder. The most popular methods are rotating ball mills and planetary mills [16]. The advantages of this method are its simplicity and low cost, while the disadvantages are agglomeration of the powders, high particle size distribution range and contamination of the powders. These methods are used for metallic and inorganic materials, but not for organic materials.

## **2.3. In situ methods**

*In situ* synthesis processes are lithography, physical and chemical vacuum deposition processes in vaporous phase, spray coatings, etc [16]. They are mostly used to manufacture nanostructured layers and coatings. Getting powders is done by spraying deposits on the collector. Nanoparticle synthesis is relatively ineffective by this method.

## **2.4. Synthesis in gaseous phase**

Synthesis in gas-phase includes flame pyrolysis, electro-explosion, laser ablation, evaporation at high temperatures and plasma synthesis techniques [16]. The main disadvantages of these techniques are extreme temperature and pressure conditions and high costs.

## **2.5. Microemulsion technique**

In contrast to the above mentioned methods, microemulsification technique has several advantages, including a better control of nanoparticle properties, such as size, geometry, morphology, homogeneity and surface area [17, 19]. In Figure 1 some of the most interesting forms of nanoparticles synthesized in water-in-oil microemulsion are presented.

This method allows the use of various combinations of aqueous phase/surfactant/organic phase (Table 1).

Microemulsion is used for the synthesis of nanomaterials with high specific surface area and structure similar to the original template, so formulating and controlling the microemulsion process have become extremely

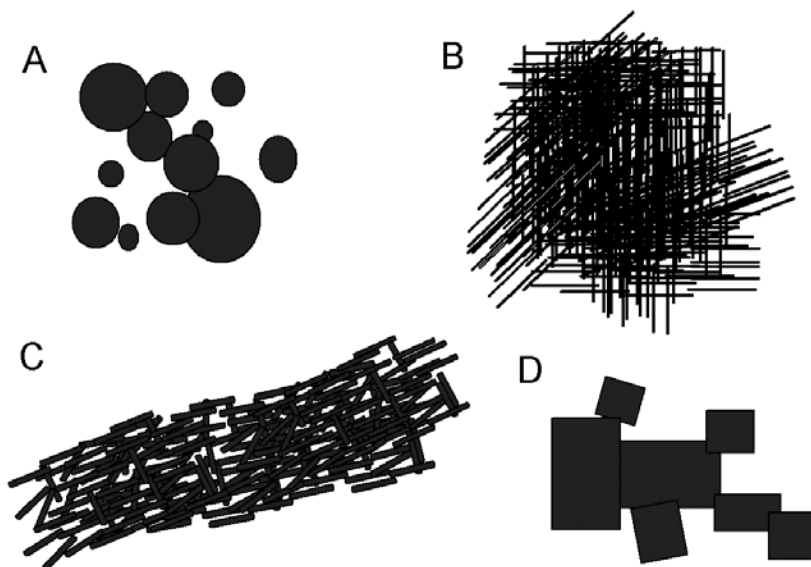


FIGURE 1

Nanoparticles generated in microemulsion: (A) spheres, (B) nanowires, (C) nanobars, (D) nanoplatelets

important for various applications. Microemulsion formulation depends on the operating conditions (temperature, pH) and the composition of the phases presented in the system. Its precise composition is extremely useful, not only to obtain microemulsion, but also for processing properties such as type, stability, viscosity and droplet size.

Microemulsions are used as synthesis nanoreactors for nanoparticles with low polydispersity. When the synthesis proceeds in a polar solvent, the areas of interest are water-in-oil, and when the process requires a non-polar phase, the areas of interest are oil-in-water. An important feature of this system is its dynamics, micelles frequently collision due to Brownian motion and merging to form dimers, exchanging components and then splitting up. This exchange process is fundamental for the synthesis of nanoparticles in microemulsion templates as allows the solubilized reagents in separate systems to react after mixing. This is for example the case of metal oxide nanoparticles in which one microemulsion contains the metal salt as aqueous phase and the other as the reducing agent. Thus, the microemulsion templates can be described as *nanoreactors* that provide a suitable environment for controlling the nucleation and growth of nanoparticles. In addition, in the final stage of nanoparticles growth, the steric stability is ensured by surfactant layer that prevents the aggregation of nanoparticles [46].

Microemulsification method has the advantage of a uniform distribution of the reducing agent which will react rapidly with the metallic

TABLE 1  
Microemulsion systems as templates for nanoparticles synthesis

NP	Surfactant	Microemulsion system	Reduction system	References
Metallic nanoparticles				
Pt	Ionic (CTAB)	W/O*	Chemical agent: N <sub>2</sub> H <sub>4</sub>	[18]
Pt, Pd	Ionic (AOT)	Isooctane/AOT/water	Chemical agent: NaBH <sub>4</sub>	[20]
		W/O CTAB/Pd(NH <sub>2</sub> ) <sub>4</sub> Cl <sub>2</sub> or K <sub>2</sub> PdCl <sub>4</sub>		
Pd	Ionic (CTAB)	/octanole	Chemical agent: N <sub>2</sub> H <sub>4</sub>	[18]
Rh	Ionic (CTAB)	W/O	Chemical agent: hydrogen	[18]
Ir	Ionic (CTAB)	W/O	Chemical agent: active hydrogen	[18]
Au	Non-ionic (Pentaethylene Glycol Dodecyl Ether (PEGDE))	W/O HAuCl <sub>4</sub> /cyclohexane/ PEGDE	Chemical agent: NaBH <sub>4</sub>	[21]
	Non-ionic (Pentaethylene Glycol Dodecyl Ether)	W/O AgNO <sub>3</sub> /n-hexane/PEGDE	Photoreduction	[22]
Au	Ionic (AOT)	W/O	Photoreduction	[22]
Au	Ionic (AOT)	W/O diethyl-ether/AOT/water	Chemical agent: dodecanthiole	[23]
Au	Ionic (CTAB)	O/W** CTAB/n-pentanol/hexane/ water	Dodecanthiol	[24]
Au	Ionic (SDS)	W/O SDS/toluene-pentanol (1:1)/ water	Chemical agent: poliethylenimine	[25]
Au, Ag	Non-ionic (Triton X-100)	W/O Triton X-100/ciclohexane/water	Chemical agent: NaBH <sub>4</sub>	[26]
Au	Ionic (SDS)	W/O	Chemical agent: poli-( <i>N,N</i> -dialile- <i>N,N</i> -dimethyl- amonium-salt- <i>N</i> -octhyl-carbox- ilate maleamic)	[27]
Au	Ionic (CTAB)	W/O CTAB/n-butanol/ n-heptane/HauCl <sub>4</sub>	Chemical agent: CTAB	[28]
Au	lauryl glucoside, lauryl fructose and lauryl ascorbate	O/W lauryl glucoside, lauryl fructose and lauryl ascorbate/toluene/apã	Microwave irradiation	[29]
Au	Non-ionic (Triton X)	O/W water/Triton X-100/hexane	Lauroyl glucose, lauroyl fructose and lauroyl ascorbate	[30]
Au	Ionic (AOT)	O/W water/AOT/ciclohexane	Lauroyl glucose, lauroyl fructose and lauroyl ascorbate	[30]

TABLE 1  
Continued

NP	Surfactant	Microemulsion system	Reduction system	References
Au	Ionic	W/O	UV photoreductive surfactant in: hexyl-phenil-azo-sulfonate	[31]
Au	Non-ionic (Brij 30)	W/O water/Brij 30/heptane	UV irradiation	[32, 33]
Re	Ionic	W/O water/AOT/n-heptane	Chemical agent: NaBH <sub>4</sub>	[34]
Cu	Ionic (Dioctyl sodium sulfosuccinate (AOT))	W/O	Chemical agent: N <sub>2</sub> H <sub>4</sub>	[35]
Metal oxide nanoparticles				
NiO	Non-ionic (rhamnolipide)	W/O water/n-heptane/rhamnolipide	Chemical agent: NH <sub>4</sub> OH	[36]
NiO	Ionic (DSS)	W/O water / sodium dodecyl sulfonate (DSS)/ n-pentanol/n-heptane	Chemical agent: NaBH <sub>4</sub>	[37]
NiO	Non-ionic (Triton X-100)	W/O water/Triton X-100/ n-hexanol/ciclohexane	Chemical agent: NaBH <sub>4</sub>	[38]
NiO, ZnO	Non-ionic (Brij 30)	W/O water/Brij 30/ organic phase	Chemical agent: NH <sub>4</sub> OH	[39]
ZnO	Ionic (CTAB)	W/O n-octane/n-butanol/CTAB/water	Chemical agent: NaOH	[40]
SnO <sub>2</sub>	Ionic (SDS)	W/O water/SDS/hexane	Chemical agent: NH <sub>4</sub> OH 6%	[41]
GeO <sub>2</sub>	Ionic (AOT)	W/O germanium tetraethoxide/AOT/ 2,2,4-trimethylpentane	Chemical agent: NaOH	[42]
SiO <sub>2</sub>	Ionic (CTAB, SDS)	W/O water/ Tetraethylorthosilicate/ ethanol/CTAB, AOT	Chemical agent: NaH <sub>3</sub>	[43]
ZrO <sub>2</sub>	Nonionic (Triton X-100)	W/O zirconium salt/Triton X-100/ ciclohexane/hexanol	Chemical agent: H <sub>2</sub> SO <sub>4</sub>	[44]
TiO <sub>2</sub>	Ionic (AOT)	W/O water/ciclohexane/AOT/ titanium tetraisopropoxide	Hydrolysis in the organic phase	[45]
Organic nanoparticles				
C <sub>60</sub>	Non-ionic (Triton X-114)	O/W Triton X-114/ water/ acetonitrile/pinus oil	Chemical agent: Acetonitrile	[11]

\*water-in-oil microemulsion (W/O)

\*\*oil-in-water microemulsion (O/W)

precursor, by coalescence and collision of the two micellar aggregates containing different reactants. Nucleation will take place in the same time in the entire mass of microemulsion, which will favor the formation of a large number of nuclei within the aqueous core of W/O final system.

Simple or combined nanoparticles are important materials in developing new equipment that can be used in numerous physical, biological, biomedical and pharmaceutical applications [47-49].

### **2.6. Microemulsion assisted sol-gel procedure**

The microemulsion assisted sol-gel technique allows the incorporation of inorganic and/or organic functional compounds into the colloidal aggregates of microemulsion, this being used as template both for the nanoparticles synthesis and for nanostructured silica network creation.

This method shows several advantages [50, 51]:

- the compatibility of the hybrid silica nanomaterials synthesized using the microemulsion method to increase the solubility of hydrophobic active compounds and to provide a stable and easy operation system for components solubilized together, probably with protection against degradation;
- the possibility to control the nanoparticles composition, size and shape with protection against agglomeration, leading to highly homogeneous and monodisperse nanomaterials;
- the reduction of secondary product formation by replacing the processes in several stages with the synthesis in initial reaction medium ("one-pot" procedure), having the advantages like less chemical consumption and nanomaterials synthesis as a film form, all of these being in accordance with the concept of green chemistry.

## **3. W/O MICROEMULSIONS – TEMPLATE FOR THE SYNTHESIS OF NANOPARTICLES**

A high number of nanomaterials were synthesized in water-in-oil microemulsions [52-56]. *Liu et al.* [57] have studied by TEM the formation of nanoparticles in water-in-oil microemulsions, as these are the most used types of microemulsions for the synthesis of nanoparticles, especially the metallic ones. In Figure 2 is shown that the nanoparticle formation starts from the interface towards the micelle core.

The nanoparticle evolution is strongly influenced by the intermicellar change rates. The size and shape are dependent of five important parameters: solvent, surfactant/cosurfactant type, reactant concentration, ionic additives, water/surfactant ratio, reaction time.

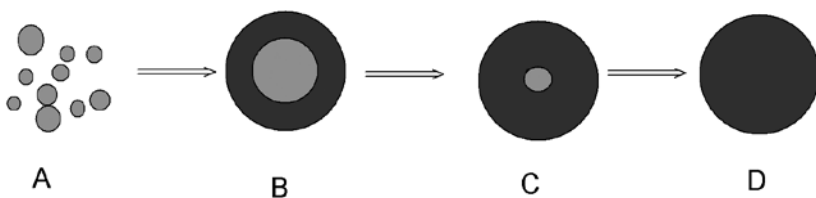


FIGURE 2

TEM images of the evolution of nanoparticles in reverse micelles at different reaction times: (A) 5 min.; (B) 30 min.; (C) 2 h; (D) 12 h from the beginning of the reaction

Therefore by controlling these parameters that influence the microemulsion and the nanoparticle formation kinetics, nanoparticles with different geometries, hollow and filled or core-shell can be synthesized.

### 3.1. Metallic nanoparticles

From all the transitional metals, gold is the most electronegative and as such it can be generated its salts using a high number of reduction agents (Table 2). Gold nanoparticles can be obtained from their precursor salts by the reduction with: hydrogen, hydrures, hydrazine, hydroxylamine, alcohols and organic species with reductive character.

*M. Faraday* was the first who studied the formation of colloidal gold solution using phosphorus ions as reducing agent  $[\text{AuCl}_4]^-$ . He investigated the optical properties of thin films prepared from colloidal solutions and observed reversible color changes of films by mechanical compression (from blue - purple to green by pressurization) [58]. Many other reducing agents easier to handle have been discovered (Table 2). Thus, meanwhile the reduction methods have been improved, particularly in terms of better control of particle size, but chemical principles are the same: reducing  $\text{Me}^{n+} \rightarrow \text{Me}^0$ .

A so-called “green chemistry” has evolved in recent years, claiming that the gold nanoparticles (AuNPs) can be generated using natural organic compounds as reducing agents [59].

An elegant and valuable method is to generate gold nanoparticles by reduction in water-in-oil microemulsions. Because of the low size of the template provided by the microemulsion, the control of nanoparticle growth can be obtained by varying the concentration of the ligand or other experimental conditions. The use of potent ligands was still a major improvement in the synthesis and manipulation of metal colloidal dispersions. In this direction phosphates and thiols were found to be much better stabilizers than citrate, as these molecules allow the isolation of gold nanoparticles as solids, which can be redispersed in suitable solvents [60]. However, it was noted that the size of the gold particles may change during the process [61].

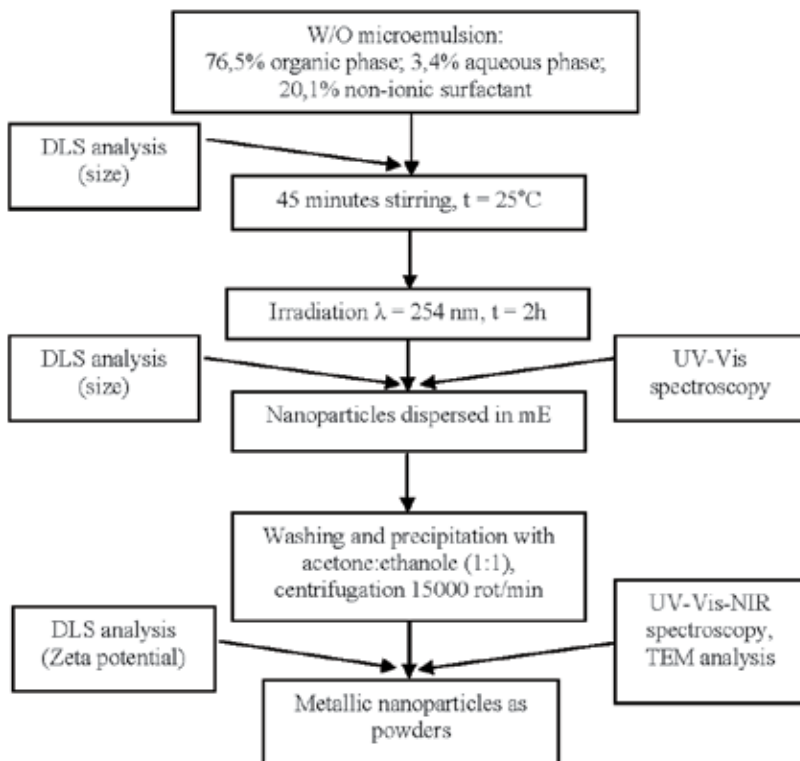
TABLE 2  
Gold nanoparticles synthesis by reduction, in different conditions

Precursor	Reduction agent	Medium	Stabilizer	Reaction conditions	D, nm	Applications
HAuCl <sub>4</sub>	Na <sub>3</sub> Cit	Water	Cit <sup>3-</sup>	RT	12-60	Biology
HAuCl <sub>4</sub>	Ascorbic acid	Water	Cit <sup>3-</sup>	RT	12	Biology
Au-arylphosphine complexes	NaBH <sub>4</sub>	Water	Arylphosphine	Inert	1	Biology
HAuCl <sub>4</sub>	Etilic alcohol	Water	-	Ultrasonication	10	Biology
HAuCl <sub>4</sub>	White P in ether	Water	-	boiling	3-5	Biology
HAuCl <sub>4</sub>	NaSCN		SCN	RT	2,6	Biology
HAuCl <sub>4</sub>	Na <sub>3</sub> Cit/ tanic acid	Water	Cit <sup>3-</sup> / tanic acid	heating	3-17	Biology
HAuCl <sub>4</sub>	NaBH <sub>4</sub>	Water	Cit <sup>3-</sup>	4°C	4	Covering
HAuCl <sub>4</sub>	NaBH <sub>4</sub>	Toluene/ Water	Thiol	RT	3	Chemistry
HAuCl <sub>4</sub>	Na <sub>3</sub> Cit/ NaBH <sub>4</sub>	Water	Cit <sup>3-</sup>	0°C	4	Covering
HAuCl <sub>4</sub>	(Ph <sub>3</sub> P) AuCl	Benzene	B <sub>2</sub> H <sub>6</sub>	-	1,4	Catalysis, sensors

Photoreduction is a very well known and widely recognized method, preferred by many researchers as it is a “clean”, convenient and rapid method for nanoparticles preparation [62-64]. This photochemical method is based on the growth of gold nanoparticles around a “crystalisation seed” under the action of light radiation [64].

Beyond the traditional methods, a new method has recently been developed, microemulsion assisted photoreduction technique (MAPR) (Scheme 1) [65], which allows high flexibility during synthesis. Being a combined method (microemulsion and photoreduction) it has the advantages of both techniques, among them one can mention:

- the reduction reaction of a precursor metal (HAuCl<sub>4</sub>) is carried out under UV radiation, thereby reducing the reagent consumption and the side effects they produce;
- the possibility of obtaining NP in both water-in-oil (W/O) and oil-in-water (O/W) microemulsions increases more the experimental versatility of this method;
- is applicable for a wide range of metal NPs, ranging from those with positive reducing potential to these with negative reducing potential or from ‘bulk’ NPs to the hollow spheres;



SCHEME 1  
Synthesis of metallic nanoparticles

- MAPR method can be fitted over a wide range of nanoparticles by simply adjusting the type or quantity of polar/non-polar phase and surfactants, allowing fine tuning of the micelle and NP diameter.

The photoreduction of  $\text{Au}^{3+}$  in different water-in-oil microemulsion systems yields spherical gold nanoparticles with diameters ranging between 2.5 and 30 nm, depending on the type of the organic phase. It also presents a good polydispersity and a very good stability (Table 3). The smallest nanoparticles (2.5 nm) were obtained with ethyl acetate (EtAc) as organic phase, which has a short carbon chain and a polar head as the carboxyl group. These characteristics make it less hydrophobic than other hydrocarbons used in Table 3. This is why, the solubilization capacity of the surfactant is lower, resulting in an increase of the repulsion forces between the chains of the surfactant, and therefore, the size of the droplet is smaller. The largest AuNP (30 nm) was obtained using the system isooctane/Brij30/HAuCl<sub>4</sub> due to the branched structure of the carbon chain of isooctane, which prevents the packing of the compact chains of surfactant at water/oil interface, resulting in a larger diameter of the droplet.

TABLE 3  
The size of AuNPs inside W/O microemulsion template

Microemulsion system	Size, nm	Polidispersity	ZP, mV
EtAc/Brij30/HAuCl <sub>4</sub>	2.5	0.21	30
C6/Brij30/HAuCl <sub>4</sub>	24.1	0.20	35
C7/Brij30/HAuCl <sub>4</sub>	9.8	0.25	51
iC8/Brij30/HAuCl <sub>4</sub>	30.0	0.30	49
C9/Brij30/HAuCl <sub>4</sub>	18.0	0.40	32

where: HAuCl<sub>4</sub> - hydrogen tetrachloroaurate; Brij 30 – polyoxyethylene 4-lauryl ether; C6 – ciclohexane; C7 – n-heptane; iC8 – isooctane; C9 – nonane; EtAc – ethyl acetate.

TEM analysis (Figure 3) of the AuNPs obtained through photoirradiation of gold precursor in C7/Brij30/HAuCl<sub>4</sub> system confirmed the spherical shape of nanoparticles. The statistical analysis indicated that the average size was around 10 nm, value also registered by DLS analysis as shown by Enachescu et al. [66].

The kinetic behavior of C7/Brij30/HAuCl<sub>4</sub> system under UVC irradiation was evaluated by electronic spectra (Figure 4) which indicated a systematic growth of 530 nm peak, attributed to the surface plasmon resonance band of monodisperse gold nanoparticles, as evidenced by Fleancu et al. [67].

### 3.2. Functionalized metallic nanoparticles

The stabilization and in the same time functionalization of AuNPs with different capping agent, such as thiols [68-72], surfactants [73,74] or polymers [75-81] became increasingly used since the functionalized metal nanoparticles are more

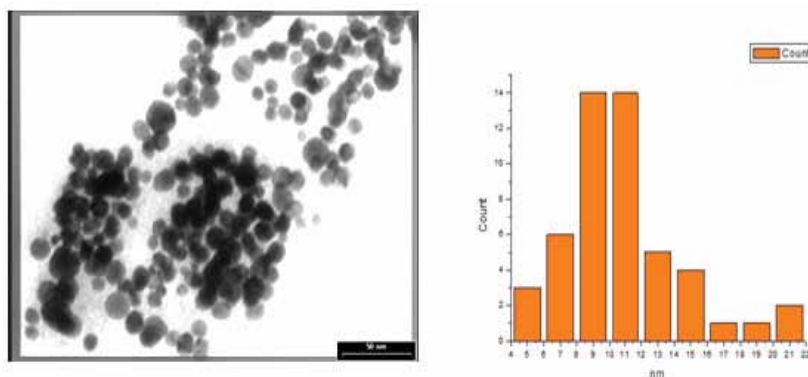


FIGURE 3  
TEM images of AuNP (left side) and the corresponding statistical distribution of their sizes (right side) in C7/Brij30/HAuCl<sub>4</sub> system. Courtesy of M. Enachescu, University Politehnica of Bucharest [66],

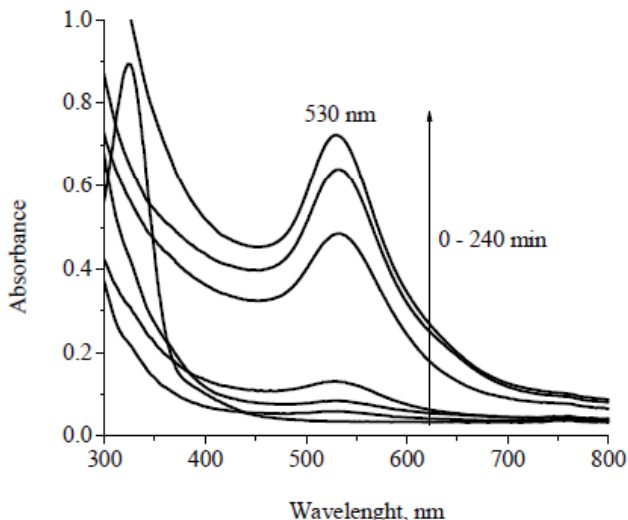


FIGURE 4

Evolution in time of AuNPs using UV-VIS electronic spectra in C7/Brij30/HAuCl<sub>4</sub> system. Courtesy of M. Fleancu, University Politehnica of Bucharest [67],

stable than those unfunctionalized, the latter being affected by van der Waals forces arising from the proximity of nanoparticles [82]. If in the solution, there is nothing to oppose these forces the nanoparticles will agglomerate leading to the reduction of the specific surface. Thiols are a class of chemical compounds that can stabilize gold nanoparticles regardless the synthesis method. Mixing the thiol with a gold precursor solution, a protector layer is formed around the nanoparticles, and by the formation of a strong covalent bond, Au – S, the interaction of the nanoparticles with each other and thus their agglomeration is prevented.

AuNPs stabilized with MS had very small sizes (10 nm), were spherical in shape and the homogeneity of AuNPs, as shown by TEM image, is consistent with the spectrum provided by DLS analysis (Figure 5).

There are only few reports in literature regarding the functionalization and stabilization of AuNPs inside W/O or O/W microemulsion [66, 83]. For example, Sodium 3-mercaptopropane sulfonate (MS) and cysteamine monochlorhydrate (CS) thiols were used to stabilize AuNP in W/O and also in O/W microemulsion, and from polymer class, oleyamine.

### 3.3. Metallic oxides nanoparticles

Hydroxide nanoparticles (Ni(OH)<sub>2</sub>, Zn(OH)<sub>2</sub>) were synthesized using the same procedure of microemulsion with the difference that in this case, the water phase consisted in an aqueous solution of a metal salt (Ni(NO<sub>3</sub>)<sub>2</sub> • 6H<sub>2</sub>O (1 M). The processing steps of the synthesis are found in Scheme 2. In order to synthesize metal oxide nanoparticles two W/O microemulsions were prepared and

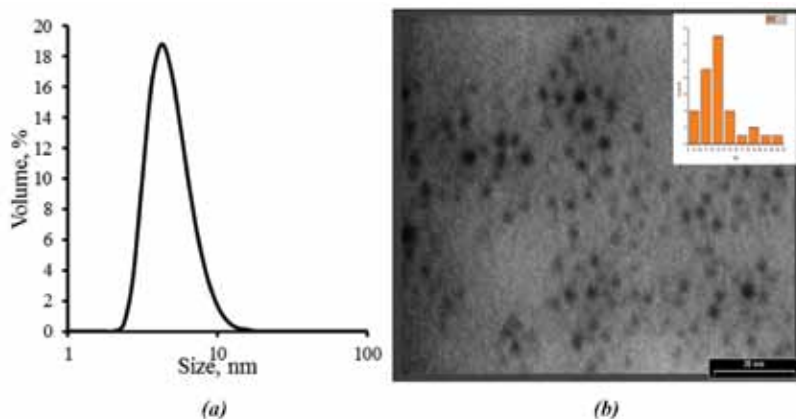


FIGURE 5 DLS spectrum (a) and TEM micrograph (b) of AuNP functionalized with sodium 3-mercaptopropane sulfonate obtained in C7/Brij30/ HAuCl<sub>4</sub> W/O microemulsion system and the statistic distribution of sizes

mixed. The first microemulsion aqueous core was formed from the electrolyte of metal salts (Ni<sup>2+</sup>) and the aqueous core of the second microemulsion by the reducing agent (NH<sub>4</sub>OH) needed to obtain the corresponding oxides.

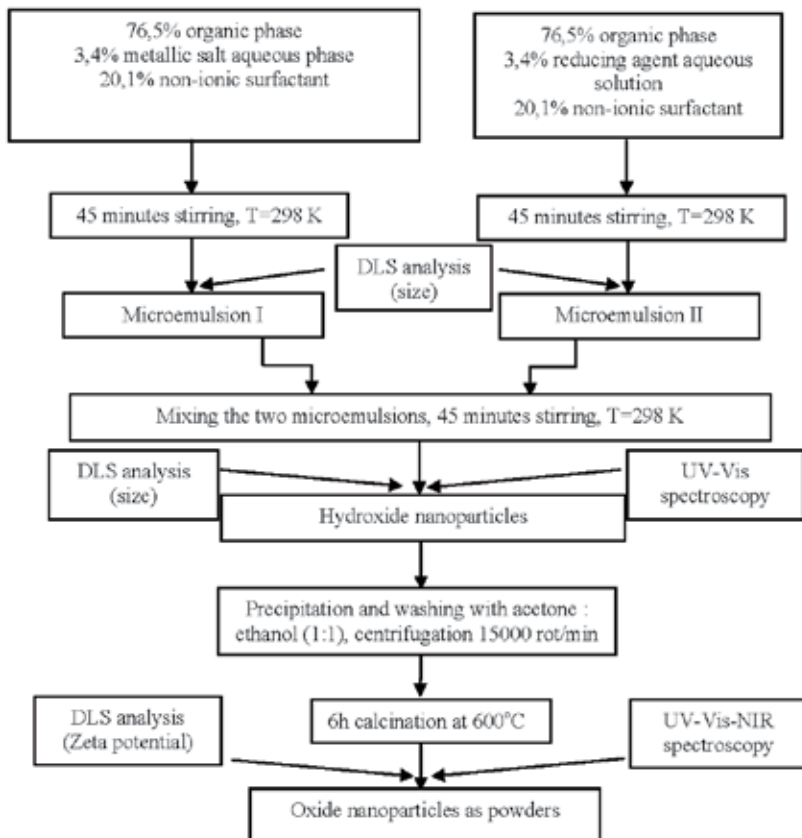
The UV-VIS spectrum of NiO nanoparticles as powders (Figure 6) identified two peaks, one at 385 nm, and the other at 650 nm. The existence of two absorption peaks in the visible region may be caused by different shape of NiO NPs formed during the nucleation process.

Meghea et al. [13] obtained NiO nanoparticles in water-in-oil microemulsion with sizes around 6 nm (Figure 7). NiO crystallites are evidenced by the diffraction image which shows 5 well-defined diffraction rings which can be indexed as (111), (200), (220), (311) and (222) crystal planes corresponding to the cubic NiO phase structure.

### 3.4. Organic nanoparticles

Fullerene, C<sub>60</sub>, is a material with outstanding physical and chemical properties that has found application in the construction of photovoltaic cells [84], filters (laser protection glasses) [85] and nonlinear optics [86]. This has been achieved by encapsulation of fullerene molecules in a matrix resistant to irradiation and aging and impermeable to oxygen molecules. C<sub>60</sub> molecules are typically insoluble in polar solvents and thus preparation of material containing fullerenes in dispersed form or simply placing them in different porous media or mesoporous become very difficult.

The microemulsion can maintain or improve the physical and chemical properties of the fullerene, and may also overcome some of the obstacles in the application of C<sub>60</sub> in material science, such as their low solubility. Thus, the property of C<sub>60</sub> to aggregate can be controlled by using a suitable microemulsion system.



SCHEME 2  
Metallic oxides synthesis chart

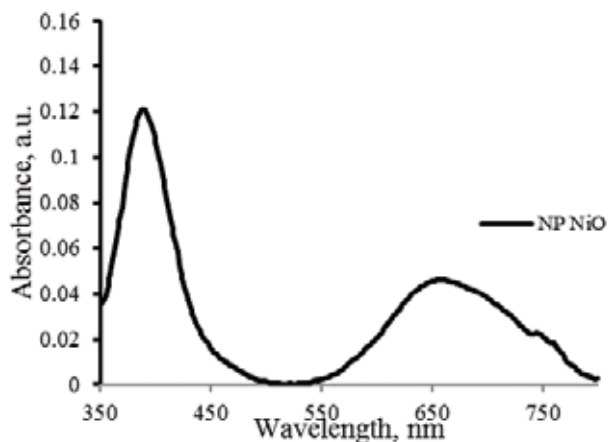


FIGURE 6  
UV-VIS spectra of NiO nanoparticles obtained in water-in-oil microemulsion

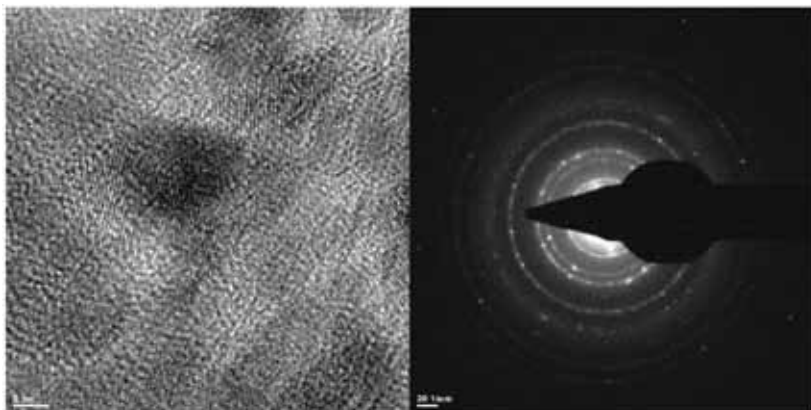


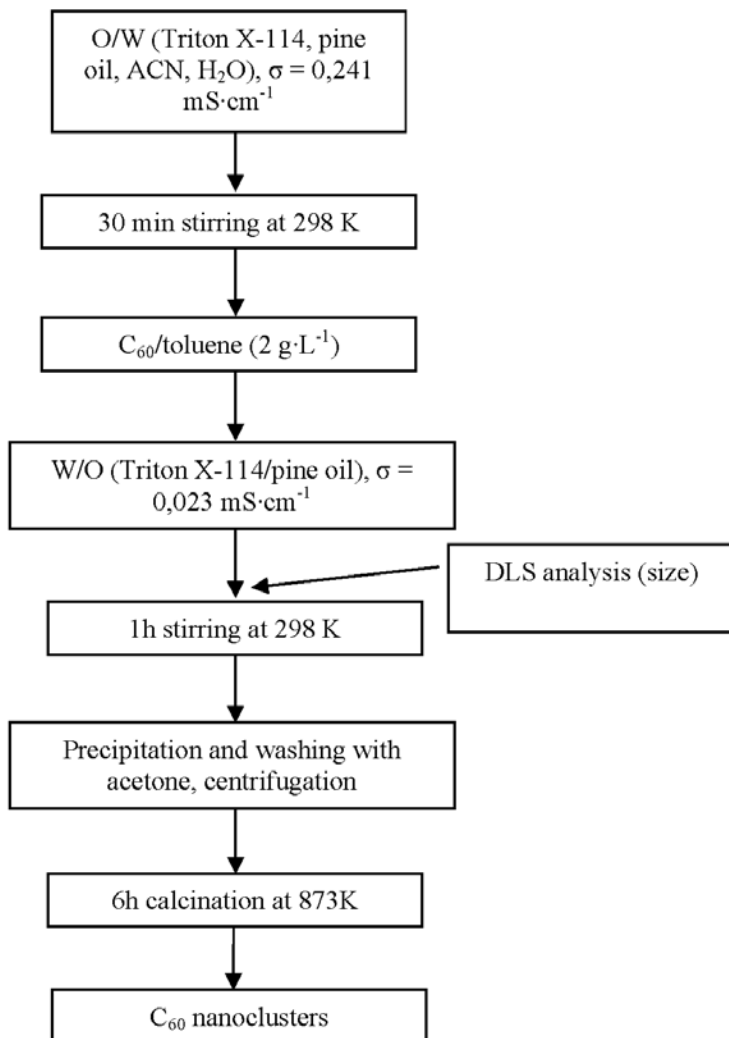
FIGURE 7  
HR-TEM micrograph of NiO NP and the corresponding electron diffraction image (SAED).  
Courtesy of A. Meghea, University Politehnica of Bucharest [13],

For the synthesis of organic nanoparticles (like  $C_{60}$  nanoclusters) an oil-in-water microemulsion was chosen with the following composition, 30 % non-ionic surfactant (Triton X-114), water: ACN (1: 1) each 10% and the remaining 50% the organic phase (pine oil) (Scheme 3) [11]. The system is suitable for the formation of toluene-in-water droplets necessary for initiating the process of clustering fullerenes in the presence of ACN.

The formation of O/W microemulsion has been supported by the value of electrical conductivity ( $\sigma = 0.251 \text{ mS} \cdot \text{cm}^{-1}$ ). After 30 minutes stirring at room temperature over the O/W microemulsion a solution of fullerene and toluene ( $2 \text{ g} \cdot \text{L}^{-1}$ ) was added so that the properties and appearance of the O/W microemulsion to be held (controlled by the value of electrical conductivity). The fullerene concentration in the system was 0.01%. In order to obtain  $C_{60}$  nanoclusters, the O/W microemulsion was added dropwise in a mixture of Triton X-114 and pine oil prior prepared. The final mixture was stirred for 1h at room temperature. The inversion of O/W microemulsion in a W/O was confirmed by different values of electrical conductivity, from  $\sigma = 0.241 \text{ mS} \cdot \text{cm}^{-1}$  to  $\sigma = 0.023 \text{ mS} \cdot \text{cm}^{-1}$ . The fullerene nanoclusters synthesis scheme was presented in Scheme 3.

HR - TEM images of  $C_{60}$  molecules and fullerene nanoclusters ( $C_{60}$  NP) are shown in Figure 8, from which it can be seen that  $C_{60}$  used in the synthesis is a buckminsterfullerene with a spherical molecular structure in which carbon atoms are positioned at the ends of a regularly truncated icosahedron composed of 20 hexagons and 12 pentagons [87]. The diameter of a single  $C_{60}$  molecule is 0.7 nm. Meghea et al. synthesized  $C_{60}$  nanoclusters (Figure 8) with sizes around 10 nm, and fullerene was in the crystalline form [11].

VIS-NIR diffuse reflectance spectra of  $C_{60}$  and  $C_{60}$  nanoclusters obtained by Meghea et al. as powders (Figure 9) showed similar features for the two materials [11]. They had a lower absorption on the left side of the visible



SCHEME 3

Schematic diagram for synthesis of organic nanoparticles ( $C_{60}$  nanoparticles)

domain until 600 nm due to a small chromophore content and higher on the right part of the visible and near infrared domains between 700 – 800 and 1400 – 2000 nm as a direct result of nanoparticles aggregation.

### 3.5. Functional materials

The importance of studying the silica based materials reached the highest level due to the extensive applications in the fields of catalysis, separation, electronic and bio-tehnology. The silica materials show several advantages, such as:

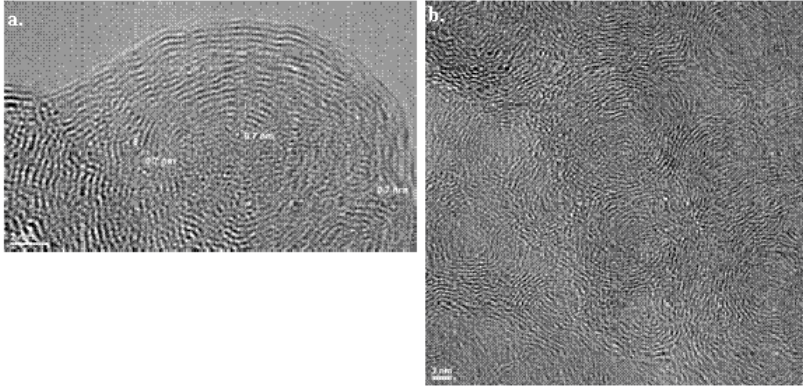


FIGURE 8  
HR-TEM images for fullerene (a) and C<sub>60</sub> nanoclusters (b). Courtesy of A. Meghea, University Politehnica of Bucharest [11].

porous structure, high specific surface area, high thermal stability, optical transparency and chemical inert structure. Nevertheless, the mesoporous materials based on pure silica present few drawbacks: low catalytic activity and nonselective adsorption properties, limitation which can be overcome by the immobili-

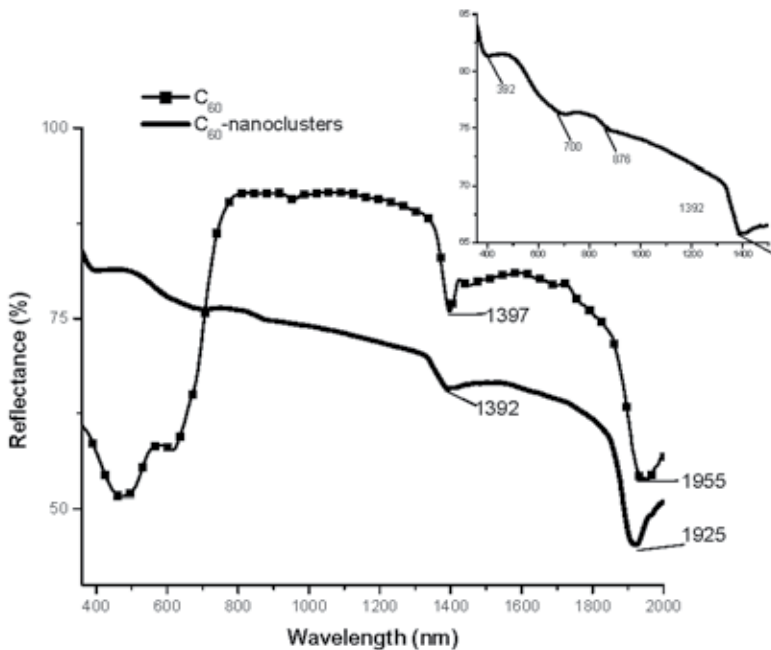
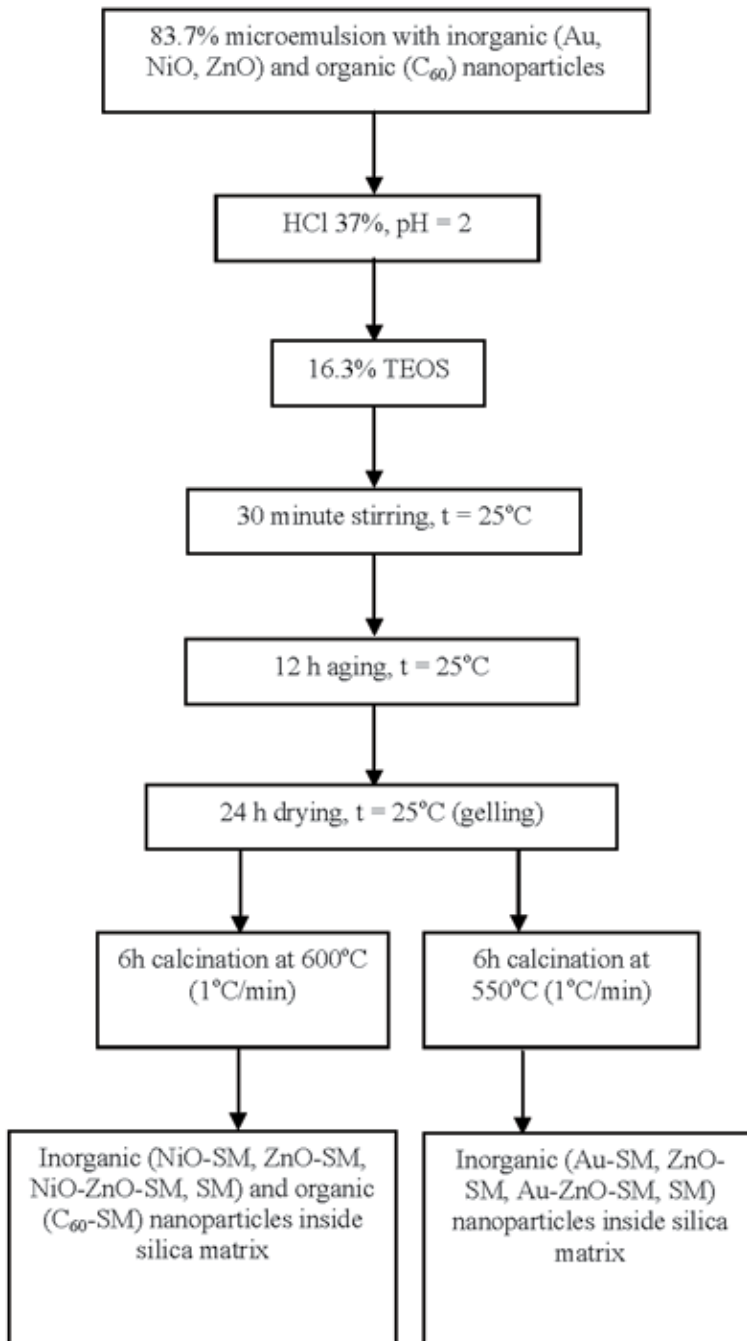


FIGURE 9  
The VIS-NIR diffuse reflectance spectra of solid C<sub>60</sub> and C<sub>60</sub> nanoclusters



SCHEME 4

Synthesis stages of inorganic and organic nanoparticles based materials embedded in silica matrix (SM)

sation of functional components in silica support. These kinds of materials combine the silica mesoporous special properties with those of functional components (metall and/or metall oxide nanoparticles, chromophores, biomolecules) leading to functional nanomaterials synthesis with specific applications.

As the uniform distribution of active components on silica surfaces is a real challenge, several procedures have been reported, such as: impregnation [88-90], grafting by L-S reaction or G-S reaction [91-94], isomorphous substitution [95, 96], molecular design dispersion approach [97, 98], template ion-exchange method [55, 56] and microemulsion assisted sol-gel technique [12, 13, 99, 100]. The last technique is related to the incorporation of inorganic and/or organic functional entities within the microemulsion colloidal aggregates, acting as templates for both nanoparticles synthesis and silica nanostructured network.

The inorganic and hybrid materials were obtained by microemulsion assisted sol-gel process through the incorporation of inorganic and organic nanoparticles inside silica matrix. Thus, after the synthesis of inorganic (Scheme 1 and Scheme 2) and organic (Scheme 3) nanoparticles the microemulsion pH was adjusted at 2 by the addition of HCl 37% followed by the addition of silica precursor (TEOS) (Scheme 4).

### 3.5.1. Inorganic functional materials

According to *Comanescu et al.* [13] the application of microemulsion template with similar structural units (size and shape) as synthesis method of NiO based nanomaterials leads to a monomodal platelet shape and size distribution of NiO nanoparticles covered by silica (Figura 10).

The most important advantages of using microemulsion assisted sol-gel process as synthesis method for silica based metallic oxide nanoparticles (NiO nanoparticles inside colloidal aggregates of microemulsion) is that it acts as template system also for silica network. The assumption of homogeneity of these materials is supported by specialized articles, for example *Piccaluga et al.* [101] showed that metallic oxide nanoparticles inside sol-gel matrix are formed mostly in the cavities matrix. Even further, by combining the microemulsion with classical sol-gel process the nanoparticles size and shape can be controlled thus obtaining a narrow size nanoparticles distribution.

The HR-TEM images (Figure 10) and the fast Fourier transform obtained from these micrographs (inset of Figure 10) have revealed the random-like array of SiO<sub>2</sub> inner pores and crystalline core structure of NiO nanoparticles, with dimensions of approximately 5 nm. This behaviour was sustained by the corresponding selected area electron diffraction (SAED), the presence of NiO crystallites being evidenced by diffraction image which shows 5 well-defined diffraction rings which can be indexed as (111), (200), (220), (311) and (222) crystal planes corresponding to the cubic phase structure [13].

The band gap energy values of silica based metallic oxide nanoparticles are less than 3 eV, thereby the capacity of these materials to adsorb visible light rises significantly. This can be attributed to the effect of NiO

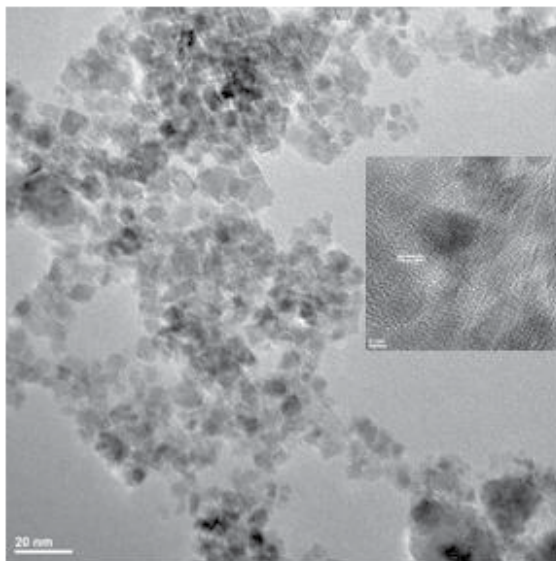


FIGURE 10

HR-TEM micrograph of NiO/SiO<sub>2</sub> nanoparticles. Courtesy of A. Comanescu, University Politehnica of Bucharest [13],

incorporation inside silica matrix which increases the number of surface oxygen vacancies and/or surface defects. Therefore by combining the properties of NiO, a p-type semiconductor and incorporation inside silica matrix, Comanescu *et al.* [13] obtained materials with band gap energy less than 3 eV (Figure 11). Thus a possible strategy to extend some semiconductor (TiO<sub>2</sub>, ZnO) absorption to visible light is the modification of its valence band position by co-catalyst coupling.

This potential photocatalytic activity of silica based NiO materials can be justified based on their ability to absorb visible or near-UV light (band gap  $\leq$  3 eV, wavelength  $>$  380 nm), after entrapment/coating into silica network, which make them biologically and chemically inert.

### 3.5.2. Hybrid functional materials

The preparation of materials that are appropriate for light-induced phenomena or solar energy conversion using fullerene-modified silica nanostructures able to absorb almost the entire visible light domain seems to be a solution for the future.

The materials obtained by sol-gel method as fullerene matrix are more advantageous than other materials since the fullerene molecules are encapsulated and covalently bounded in the new formed network. The final synthesis products are more stable as compared to polymers.

By using oil-in-water (O/W) microemulsions template based on Triton X-114/ Pinus oil/Acetonitrile/Water system fullerene C<sub>60</sub> nanoclusters embedded in sil-

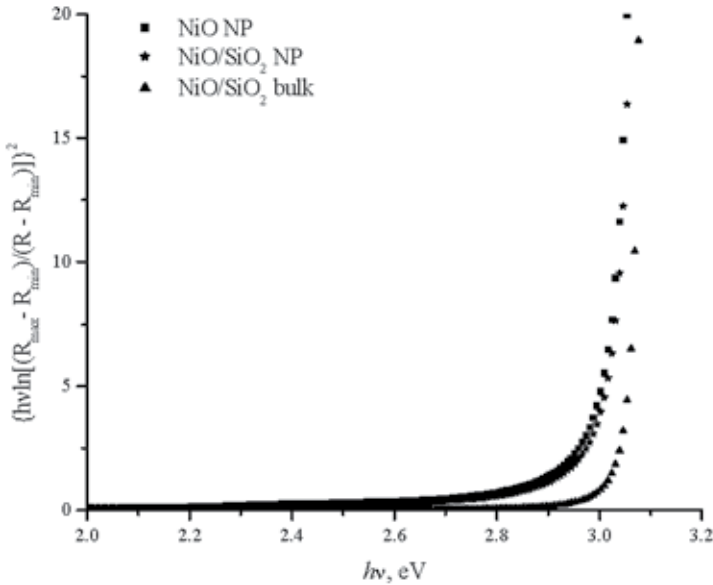


FIGURE 11

Energy band-gap determination of NiO based nanomaterials. Courtesy of A. Comanescu, University Politehnica of Bucharest [13],

ica matrix ( $C_{60}/SiO_2$  bulk) and silica coated  $C_{60}$  nanoparticles ( $C_{60}/SiO_2$  NP) have been synthesized [11]. Fullerene clusters in the size range of 10-15 nm exclusively confined inside the silica structure with wormhole like structures without a specific ordering was reported after the HR-TEM analysis [11].

It is well known that fullerene belongs to a series of carbon compounds composed only of carbon atoms, similar to diamond and graphite. Fullerene is considered a carbonaceous semiconductor material since it was firstly obtained in 1999 by arc discharged of a carbon electrode. In the crystalline form of  $C_{60}$  the molecules exhibits a band gap of 1.8 eV and after incorporating  $C_{60}$  nanoparticles (2.4 eV) inside the silica matrix semiconductors with similar bands around 3 eV have been obtained [11].

Light spectrum from infrared to ultraviolet covers a range of 0.5 to 2.9 eV. For example, the red light has energy of 1.7 eV, while the blue one, around 2.7 eV. Fullerene nanoclusters have the band gap energy of 2.4 eV and a yellow colour. By modifying the mesoporous silica insulated with fullerenes a shift of band gap values toward 3 eV was observed. This value is considered the limit that separates insulators (> 4 eV) from semiconductors (<4 eV) and therefore fullerene-modified materials fall into the category of semiconductors. By using the microemulsion (for  $C_{60}/SiO_2$  bulk) or cationic surfactant (for MCM-41) as structuring agents, the values of the band gap energies were similar, around 3 eV [11], indicating that these materials have semiconductor properties and the silica was modified with similar amounts of fullerenes.

The general pattern of spectra remains practically unchanged (Figure 12) without significant shift in peak wavelengths, but the intensity of silica bulk reflectance is increased due to the higher transparency of the silica matrix. It results that the microemulsion technique represents a method for obtaining silica coated fullerene clusters, this being the first stage of the preparation of hybrid nanocomposites appropriate for the deposition of silica based thin films.

The microemulsion assisted sol-gel technique is also used to solve another major issue, namely the incorporation of biomolecules in a suitable matrix and the preserving of their native properties. *Rau et al.* [12] had developed DNA-silica materials using the microemulsion systems as templates for sol-gel procedure as a unique approach compared to conventional methods involving adsorption on glass surface, entrapment in polymer matrix or impregnation in porous glass powders because the entrapment is based on the silica network formed around the DNA biomolecules within the microemulsion colloidal aggregates.

The preparation of DNA-silica materials consists in two steps, as shown by *Rau et al.* [12] preparation of microemulsion systems template, followed by the DNA incorporation into silica matrix (Figure 13). The atomic force (AFM) microscopy revealed an ordered units array pattern and structural units channels running parallel to each other with structural units in the DNA-silica thin films similar in size and shape (Figure 14).

## 4. APPLICATION OF NANOSTRUCTURES MATERIALS

### 4.1. Application of metal and metal oxide nanoparticles

#### 4.1.1. Coloured solar-thermal absorbers

Synthesis of nanoparticles with specific compositions, sizes, shapes and controlled dispersion and consequently special properties is very important for their applications in energy. In general, a selective solar absorber bases on the deposition of metal particles into a porous substrate, such as anodic aluminium. The porous alumina provides an ideal dielectric matrix for the nano-sized metal particles, which provides a major absorption in the solar region. Nickel pigmented aluminium oxide solar absorber was firstly reported by *Andersson et al.* [102]. It has a good optical performance (solar absorbance,  $\alpha = 0.95$  and thermal emittance,  $\epsilon = 0.12-0.20$ ) but its service lifetime can be shortened by high temperatures, humidity or atmospheric pollution. Enhancement of solar radiation absorption using a nanoparticle suspension using a nanoparticle suspension, in which Ni nanoparticles, having average diameter of 4.9 nm have much higher absorption coefficient than the base fluid over visible and near-infrared wavelengths, which are characteristic for solar radiation [103]. In addition, the absorption coefficient of the suspension in the infrared region remains the same as that of the base fluid. Nanoparticles had been also incorporated in the structure of selective solar absorbers as nano-

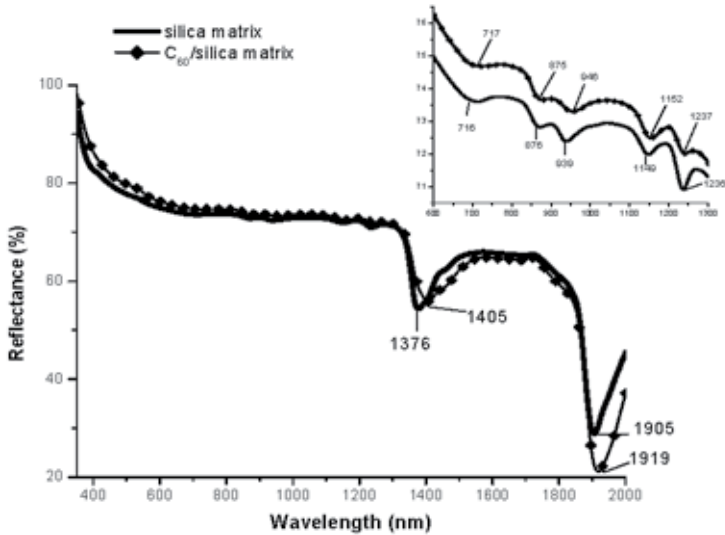


FIGURE 12. The VIS-NIR diffuse reflectance spectra of the solid silica and  $C_{60}$ /silica modified materials

metal-ceramic (cermet) or metal-semiconductor composites types [104]. NiO [105], Cr [106] or Co [107] pigmented porous alumina is a well-known selective absorber due to its high absorbance and low emittance. In the speciality literature were also reported different deposition materials from cermet class like Pt- $Al_2O_3$  [108], Ni- $Al_2O_3$  [109], Mo- $Al_2O_3$  [110], W-AlN [111], Au-MgO [112], Cr- $Cr_2O_3$  [113], etc. Nano-cermet materials can be used in the conversion of solar energy because they absorb very well the solar radiation (usually in visible) due to their quantum confinement effect also known as surface plasmon resonance phenomenon (SPR) met in the collective oscillations of conduction electrons from noble nanoparticles (Ag and Au) incorporated in a dielectric matrix [114]. The matrices used for Ag are  $SiO_2$ , ZnO,  $Bi_2O_3$ , DLC,  $Si_3N_4$ , BN,  $WO_{3-x}Al_2O_3$  [115-117]. The optical properties of nano-cermet are dependent on the size, concentration and distribution of the particles and the dielectric properties of the host matrix [114].

Solar collectors improved with metal nanoparticles, already existent in present on the market, are restrictive as colours, only shades of black and grey. In this context, using Au or metallic oxides nanoparticles based solar absorbers might overcome this drawback leading to absorbent materials with diversified colours [118]. In this direction, coloured solar selective coatings based on embedding  $Fe_2O_3$ ,  $V_2O_5$  and CuS pigments on an alumina matrix were synthesized by spray pyrolysis deposition [119]. The effects of gold nanoparticles and of the  $TiO_2$  anti-reflective thin film on the optical properties of the layers show that various red, green-yellow and dark green colours can

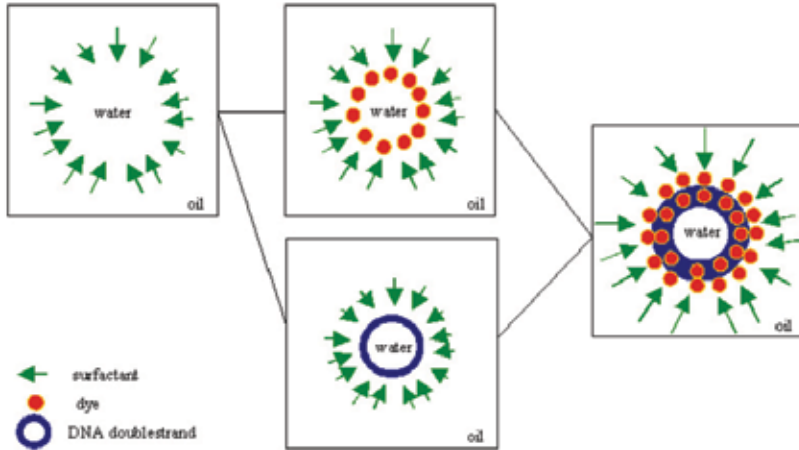


FIGURE 13

Preparation scheme of microemulsion systems applied as templates for the synthesis of DNA-silica materials. Courtesy of I. Rau, University Politehnica of Bucharest [12],

be developed as absorbers coatings with spectral selectivity up to 12. By adding gold nanoparticles, depending on the precursor type, the growth is uniform – embedding the NP in the layer, or preferentially runs on the NP, as for  $V_2O_5$ ; thus by, adequately matching the Au-NPs surface charge with that of the precursor represents a proper way for optimizing the composite structure, towards enhanced spectral selectivity.

#### 4.1.2. Biosensors

Biosensors are composed of biological molecules, such as antibodies, enzymes, carbohydrates and nucleic acids whose role is to identify and track

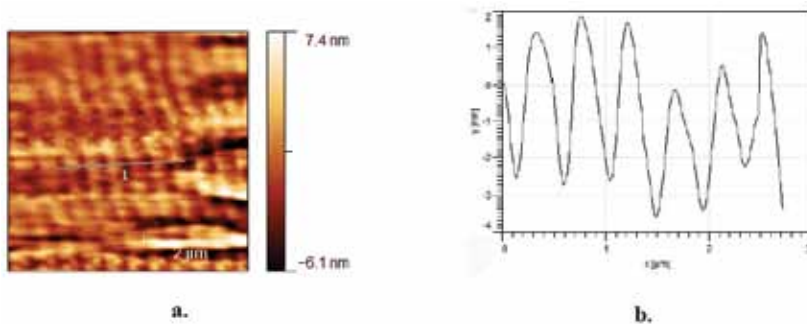


FIGURE 14

AFM micrograph (a) and surface profiles (b) of the DNA-silica thin films prepared by using the Water/TX-114/Pinus Oil as template (5000X5000 nm). Courtesy of I. Rau, University Politehnica of Bucharest [12],

the progress of any biological phenomenon of interest. Hydrogen bonding interactions, and ionic exchange between the ligand and receptor molecules coupled to different analysis techniques, such as colorimetry and fluorescence, are used for the detection of specific biochemical events. Biosensors are applicable in various fields: food industry to monitor the presence of pathogens in foods and avoiding food poisoning; environment, to detect pollutants and pesticides; medicine for the detection of viruses, bacteria and toxins, for measuring blood glucose levels.

Gold nanoparticles (AuNPs) have various applications due to their ability to provide a stable immobilization of biomolecules retaining their bioactivity, which is a major advantage for the preparation of biosensors [120]. They allow the direct electronic transfer between the redox proteins and the electrode material, and have the advantage of the absence of additional detection mediators. Additionally, they have a good biological compatibility and excellent conductivity. AuNPs used as useful interfaces for some redox electrocatalysis processes including  $O_2$ ,  $H_2O_2$ , or NADH species are present in many significant biochemical reactions. The electrochemical and electrocatalytic behaviour of a gold electrode modified by positively charged gold nanoparticles and L-cysteine film and an excellent response toward the oxidation of biomolecules such as ascorbic acid, dopamine and hydrogen peroxide was reported [121]. A potentiometric immunosensor built by means of self-assembly and opposite-charged adsorption techniques to immobilize gold nanoparticles and hepatitis B surface antibody on a platinum electrode for the detection of hepatitis B surface antigen was also reported [122]. Escosura-Muniz et al. [123] proposed an electrocatalytic device for specific identification of tumor cells through AuNPs quantification. The final detection takes into account the catalytic properties of AuNPs on hydrogen evolution for specific cell identification with a detection limit of up to 4000 cells. Combining the detection platform with various surface functionalized nanoparticles, further applications are possible for biomedical diagnosis. The additional use of magnetic nanoparticles can facilitate the signal amplification for DNA or protein detection in [124, 125].

Thiol functionalized AuNPs prepared using microemulsion assisted photoreduction procedure showed a good electrocatalytic response towards hydrogen evolution reaction in acidic medium [126]. A very good linearity of the cathodic current at a certain applied cathodic potential (of -1V vs. Ag ref.) against gold nanoparticles concentration has been determined for thiol functionalized AuNPs using sodium 3-mercaptopropane sulfonate. The obtained results are a good premise to develop further an easy-to-use biosensor for the identification and quantification of targeted metallic NPs toward specific cells (e.g. blood circulating inflammatory cells and tumour metastatic cells).

The advantages of using nanoparticles versus classical formulations are numerous, such as: ensuring better protection of biological induced degradation, increased bioavailability, and intracellular penetration. By applying nanotechnology increases efficacy, specificity, tolerability and therapeutic index of active substances.

## 4.2. Application of inorganic and hybrid functional materials

### 4.2.1. Photocatalysis field

Heterogeneous photocatalysis is a process that involves the irradiation of a metal semiconductor to produce photo-excited  $e^-$  ( $e$ ) and positively charged holes  $h^+$  ( $h$ ). The photo-excitation of semiconductor particles by light irradiation with a higher energy than its electronic band gap generates excess electrons in the conduction band ( $e^-_{cb}$ ) and an electron vacancy in the valence band ( $h^+_{vb}$ ). These photo-generated electrons and holes migrate to surfaces which participate in redox reaction generating reactive species such as hydroxyl radicals. The photogenerated electrons and holes recombine with release of photons, the recombination process has a faster kinetics than surface redox reaction and reduces the quantum efficiency of photocatalyst which represents a major drawback of the process.

This problem can be solved by the encapsulation of pre-synthesized metal oxide nanoparticles in silica support (microemulsion assisted sol-gel process); the high porosity of amorphous silica materials offers the three dimensional space required for incorporating inorganic or organic nanoparticles, which allows the components inside silica matrix to preserve their original optic and magnetic properties.

Several studies reported the application of metal oxide (NiO) and organic ( $C_{60}$ ) nanoparticles incorporated in silica matrix for the photodegradation of cationic dyes (Crystal Violet, Methylene Blue) from wastewater [13, 15, 127]. For example, the aqueous solution of cationic Crystal Violet dye was degraded by Comanescu *et al.* in the presence of photocatalyst NiO-SiO<sub>2</sub> in 21 minutes under UVC ( $\lambda = 254$  nm) light irradiation with a 30 % efficiency (Figure 15) [13]. In the case of aqueous solution of Methylene blue dye the photodegradation occurs in 6 h under UVA ( $\lambda = 365$  nm) light irradiation, the efficiency of this process being 81 % [15]. Bors *et al.* [127] demonstrated that Fullerene modified silica particles ( $C_{60}$ -SiO<sub>2</sub>) exhibits photocatalytic activity under UVC and VIS light irradiation domains. The photodegradation of Methylene Blue takes place with 85 % and 40 % efficiencies under UVC and VIS light irradiation, respectively (Figure 16).

In addition to the catalysis applications, the nanocrystalline monomodal NiO prepared by microemulsion assisted sol-gel process can be also considered as a potential candidate for a multitude of applications, such as battery cathodes, electrochromic films, p-type transparent conducting films, magnetic materials, gas sensors, active optical fibers, solid oxide fuel cells electrodes.

### 4.2.2. Optical field

The investigation of nonlinear optical (NLO) properties of DNA-silica matrix (organic-inorganic) hybrid materials are of substantial interest in terms of creating low-temperature technology for optical fiber production, as well as for other important photonic applications. Silica is an excellent matrix for hybridization with func-

tional molecules and nanomaterials which can provide the necessary optical properties in order to match the requirements of specific photonic applications.

The fluorescent dye (such as Rhodamine B) can bind to double helical DNA (Figure 17) by intercalation or groove binding, reducing the fluorescence quenching caused by aggregation or the rate of the nonradiative transition from the excited state as shown by Sahraoui et al. [128].

The NLO properties of DNA-silica materials were analyzed by THG Maker fringes technique (Figure 18). The samples have been found to be THG efficient, while the nonlinear optic signal was highly dependent upon the incidence angle of of the laser beam with respect to the sample.

## SUMMARY

Microemulsions are a unique class of colloidal systems having novel properties because of their high degree of dispersion, their very low size and good enough potential to control the chemical reaction.

Comprehensive information and tools required for the design and synthesis of inorganic and hybrid silica-based nanomaterials, nanoparticles or films, using silica-microemulsion templates, are provided by the present work.

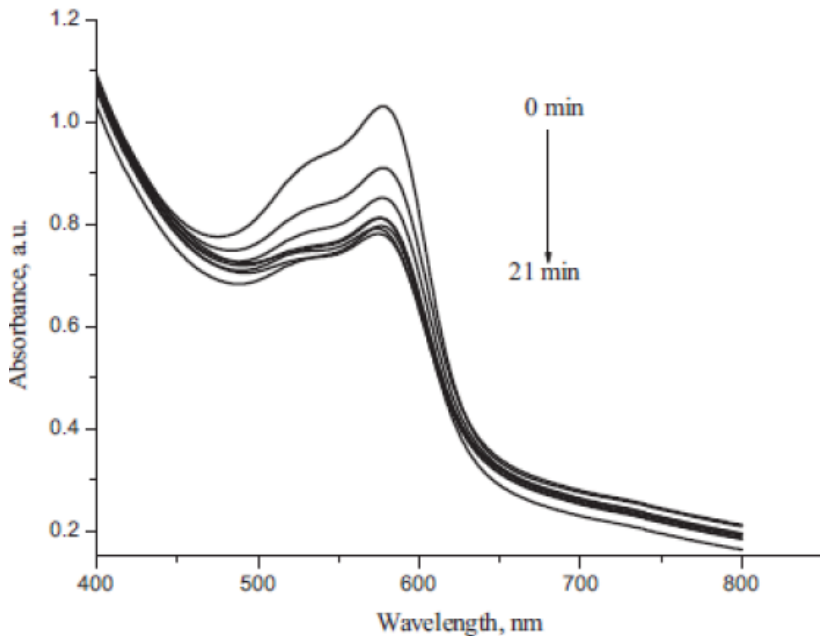


FIGURE 15

The absorption spectrum of crystal violet ( $10 \text{ mg}\cdot\text{L}^{-1}$ ) aqueous solution with NiO/SiO<sub>2</sub> NP. Courtesy of A. Comanescu, University Politehnica of Bucharest [13],

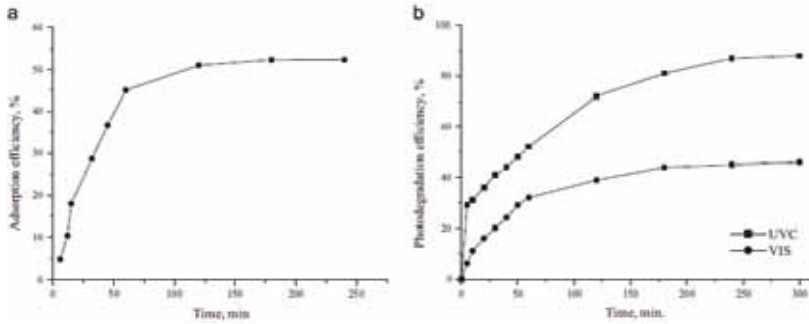


FIGURE 16

Effect of contact time on adsorption (a) and photodegradation of MB (b) on  $C_{60}/SiO_2$ . Courtesy of A. Bors, National Institute for Research & Development in Environmental Protection [127],

The microemulsion assisted sol-gel technique has some important strong points as: (i) the suitability for hybrid silica nanomaterials synthesis using microemulsion to enhance the solubility of hydrophobic active compounds and to provide a readily controlled, stable medium for the solubilized components, together, perhaps, with protection against deg-

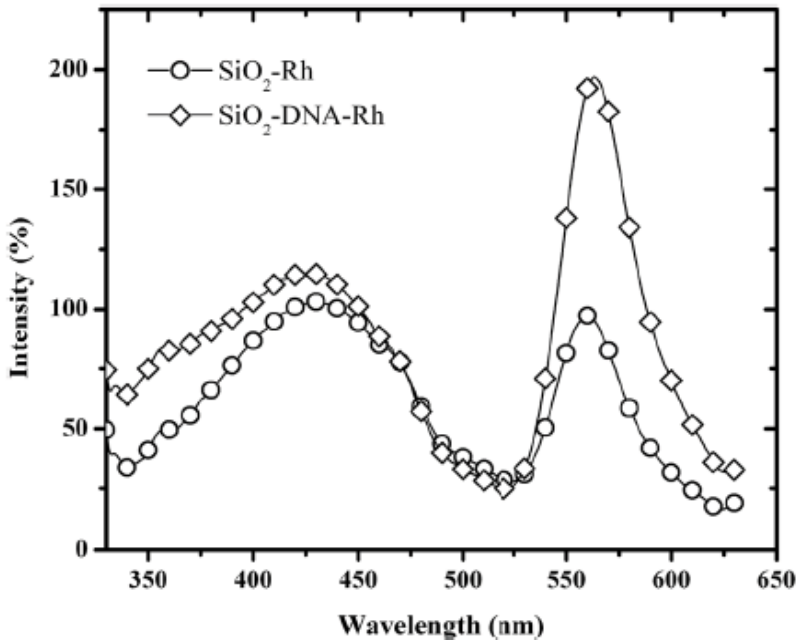


FIGURE 17

Fluorescence spectra of rhodamine-silica thin films in absence/presence of DNA. Courtesy of B. Sahraoui, University of Angers [128],

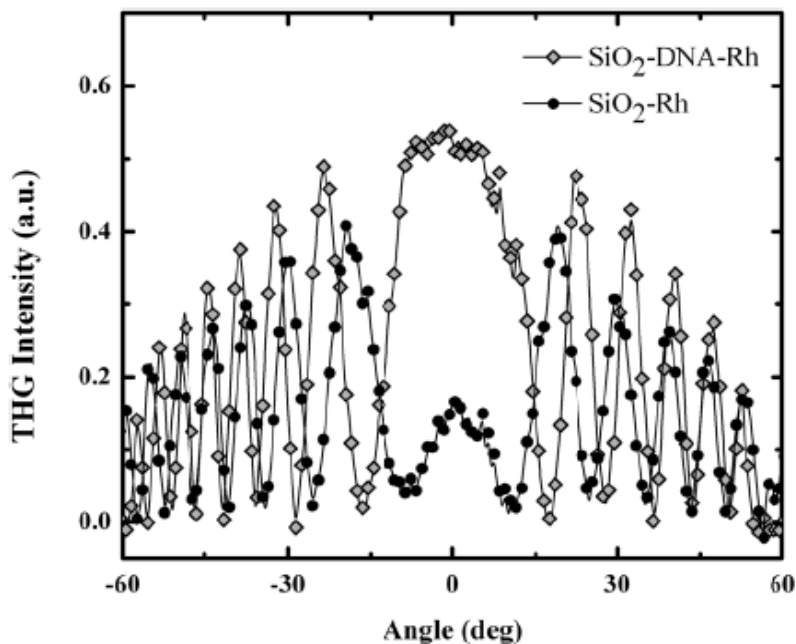


FIGURE 18

An example of the THG Maker fringes signal as a function of the incident angle in the case of the silica-Rh and silica-DNA-Rh system. Courtesy of B. Sahraoui, University of Angers [128],

radation; (ii) the possibility to control the composition, size and shape of nanoparticles and to avoid their aggregation, resulting into a high degree of homo-geneity and monodispersity of the final material; (iii) the minimization and/or managing by-products by replacing multistep processes by direct schemes, reducing effluents (solvents) and processing the final materials as films, all of them being in agreement with the Green Chemistry concept.

## REFERENCES

- [1] Pitkethly M. J., *Nanomaterials – the driving force in NanoToday*, (2004)20–29.
- [2] Chan W. C. W., Maxwell D. J., Gao X., Bailey R. E., Han M., Nie S., Luminescent quantum dots for multiplexed biological detection and imaging, *Curr. Opin. Biotechnol.*, **13**, (2002)40–46.
- [3] Brigger I., Dubernet C., Couvreur P., Nanoparticles in cancer therapy and diagnosis, *Adv. Drug. Deliver. Rev.*, **54**, (2002)631–651.
- [4] Zaheer Z., Malik M. A., Al-Nowaiser F. M., Khan Z., Preparation of silver nanoparticles using tryptophan and its formation mechanism, *Colloids Surf. B. Biointerfaces*, **81**, (2010)587–592.
- [5] Sileikaite A., Prosycevas I., Puiso J., Juraitis A., Guobiene A., Analysis of silver nanoparticles produced by chemical reduction of silver salt solution, *J. Mater. Sci.*, **12**, (2006)4–9.

- [6] Ahmad N., Malik M. A., Al-Nowaiserb F. M., Khan Z., A kinetic study of silver nanoparticles formation from paracetamol and silver(I) in aqueous and micellar media, *Colloids Surf. B. Biointerface*, **78**, (2010)109–114.
- [7] Sun X., Luo Y., Preparation and size control of silver nanoparticles by a thermal method, *Mater. Lett.*, **59**, (2005)3847–3850.
- [8] Shao K., Yao J. N., Preparation of silver nanoparticles via a non-template method, *Mater. Lett.*, **60**, (2006)3826–3829.
- [9] Li Y., Kim N., Lee E. J., Cai W. P., Cho S. O., Synthesis of silver nanoparticles by electron irradiation of silver acetate, *Nucl. Instr. Meth. Phys. Res. Section B*, **251**, (2006)425–428.
- [10] Tsuhi T., Iryo K., Watanabe N., Tsuhi M., Preparation of silver nanoparticles by laser ablation in solution: influence of laser wavelength on particle size, *Appl. Surf. Sci.*, **202**, (2002)80–85.
- [11] Mihaly M., Rogozea A., Comănescu A., Vasile E., Meghea A., Microemulsion assisted sol-gel procedure for nanostructured C<sub>60</sub> silica-based materials synthesis, *J. Optoelectron. and Adv. M.*, **10** (10), (2010)2097-2105.
- [12] Mihaly M., Comanescu A., Rogozea A., Pirvu C., Rau I., Biomaterials based on DNA embedded in silica matrix, *J. Soc. Photo-Opt. Ins.*, (2009), doi:10.1117/12.828853.
- [13] Mihaly M., Comanescu A. F., Rogozea A. E., Vasile E., Meghea A., NiO-silica based nanostructured materials obtained by microemulsion assisted sol-gel procedure, *Mat. Res. Bull.*, **46**(10), (2011)1746-1753.
- [14] Mihaly M., Lacatusu I., Enesca I. A., Meghea A., Hybride nanomaterials based on silica coated C<sub>60</sub> clusters obtained by microemulsion technique, *Mol. Cryst. Liq. Cryst.*, **483**, (2008)205-215.
- [15] Ali A. M., Majmy R., Structural, optical and photocatalytic properties of NiO-SiO<sub>2</sub> nanocomposites prepared by sol-gel technique, *Catal. Today*, **208**, (2013)2-6.
- [16] Ghorbani H. R., A review of methods for synthesis of Al nanoparticles, *Orient. J. Chem.*, **30** (4), (2014)1941-1949.
- [17] Hu A., Yao Z., Yu X., Phase behavior of a sodium dodecanol allyl sulfosuccinic diester/n-pentanol/methyl acrylate/butyl acrylate/water microemulsion system and preparation of acrylate latexes by microemulsion polymerization, *J. Appl. Polym. Sci.*, **113**, (2009)2202–2208.
- [18] Pilemi M. P., Nanocrystals: fabrication, organization and collective properties, *C. R. Chim.*, **6**, (2003)965–978.
- [19] Eastoe J., Hollamby M. J., Hudson L., Recent advances in nanoparticle synthesis with reversed micelles, *Adv. Colloid Interfac.*, 128–130, (2006)5–15.
- [20] Noh J. H., Meijboom R., Synthesis and catalytic evaluation of dendrimer-templated and reverse microemulsion Pd and Pt nanoparticles in the reduction of 4-nitrophenol: The effect of size and synthetic methodologies, *Appl. Catal. A: Gen.*, **497**, (2015)107–120.
- [21] Boutonnet M., Kizling J., Stenius P., Maire G., The preparation of monodisperse colloidal metal particles from microemulsions, *Colloid. Surface.*, **5**, (1982)209–225.
- [22] Barnickel P., Wokaum A., Synthesis of metal colloids in inverse microemulsions, *Mol. Phys.*, **69**, (1990)1–9.
- [23] Pilemi M., Lisiecki I., Nanometer copper metallic particles synthesis in reverse micelles, *Colloids Surf. A*, **80**, (1993)63–68.
- [24] Manna A., Imaea T., Yogob T., Aoic K., Okazakic M., Synthesis of gold nanoparticles in a Winsor II type microemulsion and their characterization, *J. Colloid Interface Sci.*, **256**, (2002)297–303
- [25] Chen F., Xu G. Q., Hor T. S., Preparation and assembly of colloidal gold nanoparticles CTAB-stabilized reverse microemulsion, *Mater. Lett.*, **57**, (2003)3282–3286.
- [26] Note C., Kosmella S., Koetz J., Poly(ethyleneimine) as reducing and stabilizing agent for the formation of gold nanoparticles in w/o microemulsions, *Colloids Surf. A.*, **290**, (2006)150–156.
- [27] Pal A., Shah S., Devi S., Preparation of silver, gold and silver–gold bimetallic nanoparticles in w/o microemulsion containing TritonX-100, *Colloids Surf. A.*, **302**, (2007)483–487.

- [28] Note C., Koetz J., Wattedled L., Laschewsky A., Effect of a new hydrophobically modified polyampholyte on the formation of inverse microemulsions and the preparation of gold nanoparticles, *J. Colloid Interface Sci.*, **308**, (2007)162–169.
- [29] Shen M., Du Y., Yang P., Jiang L., Morphology control of the fabricated hydrophobic gold nanostructures in W/O microemulsion under microwave irradiation, *J. Phys. Chem. Solids.*, **66**, (2005)1628–1634.
- [30] Rajput R., Kumar A. R., Zinjarde R., A simple microemulsion based method for the synthesis of gold nanoparticles, *Mater. Lett.*, **63**, (2009)2672–2675.
- [31] Spirin M. G., Brichkin S. B., Razumov V. F., Synthesis and Stabilization of Gold Nanoparticles in Reverse Micelles of Aerosol OT and Triton X-100, *Colloid J.*, **67**(4), (2005)485–490.
- [32] Vesperinas A., Eastoe J., Jackson S., Wyatt P., Light-induced flocculation of gold nanoparticles, *Chem. Commun.*, **5**, (2007)3912–3914.
- [33] Mihaly M., Fleancu M. C., Olteanu N. L., Bojin D., Meghea A., Enachescu M., Synthesis of Gold Nanoparticles by Microemulsion Assisted Photoreduction Method, *C. R. Chim.*, **15**(11-12), (2012)1012-1021.
- [34] Bedia L., Calvo J., Lemus A., Quintanilla J.A., Casas A.F., Mohedano J.A., Zazo J.J., Rodriguez M.A., Gilarranz, Colloidal and microemulsion synthesis of rhenium nanoparticles in aqueous medium, *Colloids Surf. A.*, **469**, (2015)202–210.
- [35] Pilemi M. P., Control of the size and shape of inorganic nanocrystals at various scales from nano to macromolecules, *J. Phys. Chem., C* **111**, (2007)9019–9038.
- [36] Palamisany P., Raichur A.M., Synthesis of spherical NiO nanoparticles through a novel biosurfactant mediated emulsion technique, *Mat. Sci. Eng. C Biomimetic Supramolecular Systems*, **29**, (2009)199-204.
- [37] Iijima S., Helical microtubules of graphitic carbon, *Micropor. Mesopor. Mat.*, **61**(1), (1991)273-282.
- [38] Lagergren S., About the Theory of So-Called Adsorption of Soluble Substances, *Handlinger.*, **24**(2), (1898)1-39.
- [39] Liu S., Han M. Y., Silica – coated metal nanoparticles, *Chem. Asian J.*, **5**, (2010) 36-45.
- [40] Wang Y., Zhang X., Wang A., Li X., Wang G., Zhao L., Synthesis of ZnO nanoparticles from microemulsions in a flow type microreactor, *Chem. Eng. J.*, **235**, (2014)191–197.
- [41] Zamand N., Nakhaei Pour A., Reza Housaindokht M., Izadyar M., Size-controlled synthesis of SnO<sub>2</sub> nanoparticles using reverse microemulsion method, *Solid State Sci.*, **33**, (2014)6-11.
- [42] Kawai T., Usui Y., Kon-No K., Synthesis and growth mechanism of GeO<sub>2</sub> particles in AOT reversed micelles, *Colloids Surf. A*, **149**(1), (1999)39-47(9).
- [43] Stanleya R., Samson Nesarajb A., Effect of Surfactants on the Wet Chemical Synthesis of Silica Nanoparticles, *Int. J. Appl. Sci. Eng.* 2014, **12**, 1: 9-21.
- [44] Yang X. F.; Li W. B. Preparation of Zirconia Nanoparticles in Reverse Microemulsion, *J. Acta Phys. Chim. Sin.*, 2002, **18**(01):5-9. doi: 10.3866/PKU.WHXB20020102.
- [45] Hosseini Zori M., Synthesis of TiO<sub>2</sub> Nanoparticles by Microemulsion/Heat Treated Method and Photodegradation of Methylene Blue, *J. Inorg. Organomet. Polym. Mat.*, **21**(1), (2011)81-90.
- [46] Malik M. A., Wani M. Y., Hashim M. A., Microemulsion method: a novel route to synthesize organic and anorganic nanomaterials: 1<sup>st</sup> Nano Update, *Arabian J. Chem.*, **5**(4), (2012)397-417.
- [47] Brigger I., Dubernet C., Couvreur P., Nanoparticles in cancer therapy and diagnosis, *Adv. Drug Delivery Rev.*, **54**, (2002)631–651.
- [48] Sondi I., Siiman O., Matijevic E., Preparation of aminodextran-CdS nanoparticle complexes and biologically active antibody aminodextran-CdS nanoparticle conjugates, *Langmuir*, **16**, (2000)3107–3118.
- [49] Bandow S., Kimura K., Konno K., Kitahara A., Magnetic properties of magnetite ultra-fine particles prepared by W/O microemulsion method, *Jpn J. Appl. Phys.*, **26**, (1987)713–717.

- [50] Mihaly M., Lacatusu I., Olteanu N.L., Meghea A., A systematic methodology to design silica templates: silica microemulsion formulation and nanodroplets type and size, *C.R. Chimie* **17**, (2014)342-351.
- [51] Olteanu N. L., Meghea A., Microemulsion-based silica templates for multifunctional nanomaterials, *U.P.B. Sci. Bull., Series B*, **75**, (2013)79-89.
- [52] Ayyup P., Multani M., Barma M., Palkar V. R., Vijayaraghavan R., Size induced structural phase transitions and hyperfine properties of microcrystalline Fe<sub>2</sub>O<sub>3</sub>, *J. Phys. C: Solid State Phys.*, **21**, (1988)2229–2245.
- [53] Hou M. J., Shah D. O., Interfacial phenomena in biotechnology and materials processing, Y.A. Attia, (Ed.), Elsevier, Amsterdam, 2008
- [54] Lal M., Chhabara V., Ayyub P., Maitra M. A., Preparation and characterization of ultrafine TiO<sub>2</sub> particles in reverse micelles by hydrolysis of Ti-DEHSS, *J. Mater. Res.*, **13**, (1998)1249–1254.
- [55] Zhang X., Chan K. Y., Microemulsion synthesis and electrocatalytic properties of platinum-cobalt nanoparticles, *J. Mater. Chem.*, **12**, (2002)1203–1206.
- [56] Li L., Qing-Sheng W., Ya-Ping D., Pei-Ming W., Formation and photoelectric properties of ZnSe, *Mater. Lett.*, **59**, (2005)1623-1629.
- [57] Faraday M., Philosophical Transactions of the Royal Society, London, 1857.
- [58] Schmid G., Clusters and Colloids—From Theory to Applications, Wiley-VCH, Weinheim, Germany, 1994.
- [59] Slot J. W., Geuze H. J., A new method for preparing gold probes for multiple labeling cytochemistry, *Eur. J. Cell Biol.*, **38**, (1985)87-94.
- [60] Warner M. G., Reed S. M., Hutchison J. E., Small, Water-soluble, Ligand-stabilized Gold Nanoparticles Synthesized by Interfacial Ligand Exchange Reactions, *Chem. Mater.*, **12**, (2000)3316-3320.
- [61] Sau T. K., Pal A., Jana N. R., Wang Z. L., Pal T., Size Controlled Synthesis of Gold Nanoparticles Using Photochemically Prepared Seed Particles, *J. Nanopart. Res.*, **3**(5), (2001)257-261.
- [62] Dong S., Tang C., Zhou H., Zhao H., Photochemical Synthesis of Gold Nanoparticles by the Sunlight Radiation using a Seeding Approach, *Gold Bull.*, **37**(6), (2004)3–4.
- [63] Hao W., Yang W., Huang W., Zhang G., Wu Q., Time evolution of gold nanoparticles in HPC solution after UV irradiation, *Mater. Lett.*, **62**(11), (2008)3106–3109.
- [64] Dong S., Tang C., Zhou H., Zhao H., Photochemical Synthesis of Gold Nanoparticles by the Sunlight Radiation using a Seeding Approach, *Gold Bull.*, **37**, (2004)5–8.
- [65] Rosano H. L., Clause M., *Microemulsion Systems*, Marcel Dekker, 1987.
- [66] Mihaly M., Fleancu M. C., Olteanu N. L., Bojin D., Meghea A., Enachescu M., Synthesis of Gold Nanoparticles by Microemulsion Assisted Photoreduction Method, *C. R. Chim.*, **15**(11-12), (2012)1012-1021.
- [67] Fleancu M., Olteanu N. L., Lazar C. A., Meghea A., Mihaly M., Controlled Size Gold Nanoparticles Obtained by Tuning Synthesis Parameters in Microemulsion Templates, *Rev. Chim.*, **64**(7), (2013)729-732.
- [68] Nichich N. M., Voitekovich S. V., Shavel A., Lesnikovich A. I., Ivashkevich O. A. 1-Substituted 5-thiotetrasoles as novel capping agent for stabilization of gold nanoparticles. *Polyhedron*, **28**, (2009)3138–3142.
- [69] Shi W., Sahoo Y., Swihart M. T. Gold nanoparticles surface-terminated with bifunctional ligands, *Colloid. Surface. A.*, **246**, (2004)109–113.
- [70] Kumar A., Mandal S., Suju P. M., Selvakannan P. R., Mandale A. B., Ragunath V. C., Murali S., Benzene- and anthracene-mediated self-assembly of gold nanoparticles at the liquid-liquid interface, *Langmuir*, **18**, (2002)6478–6483.
- [71] Tom R. T., Suryanarayannan V., Reddy P. G., Baskaran S., Pradeep T., Ciprofloxacin-protected gold nanoparticles, *Langmuir*, **20**, (2004)1909–1914.
- [72] Misra T. K., Chen T. S., Liu C. Y., Phase transfer of gold nanoparticles from aqueous to organic solution containing resorcinarene, *J. Colloid. Interf. Sci.*, **15**, (2006)584–588.
- [73] Samal A. K.; Sreeprasad S. T.; Predeep T. Investigation of the role of NaBH<sub>4</sub> in the chemical synthesis of gold nanorods, *J. Nanopart. Res.*, **12**, (2010)1777–1786.

- [74] Zhang L., Sun X., Song Y., Jiang X., Dong S., Wang E., Didodecyldimethylammonium bromide lipid bilayer-protected gold nanoparticles: synthesis, characterisation, and self-assembly, *Langmuir*, **14**, (2006)2838–2843.
- [75] Pimpang P., Sutham W., Mangkornong N., Mangkornong P., Choopun S. Effect of stabilizers on preparation on silver and gold nanoparticles using grinding method, *Chiang Mai J. Sci.*, **35**, (2008)250–257.
- [76] Wang W., Chen Q., Jiang C., Yang D., Liu X., Xu S., One-step synthesis of biocompatible gold nanoparticles using gallic acid in the presence of poly-(N-vinyl-2-pyrrolidone), *Colloid. Surface. A.*, **301**, (2007)73–79.
- [77] Tang X. L., Jiang P., Ge G. L., Tsuji M., Xie S. S., Guo Y. J., Poly-(N-vinyl-2-pyrrolidone) (PVP)-Capped dendritic gold nanoparticles by a one-step hydrothermal route and their high SERS effect, *Langmuir*, **24**, (2008)1763–1768.
- [78] Jiang G., Wang L., Chen T., Yu H., Chen C., Preparation of gold nanoparticles in the presence of poly(benzylether) alcohol dendrones, *Mater. Chem. Phys.*, **98**, (2006)76–82.
- [79] Tang Q., Cheng F., Lou X. L., Liu H. J., Chen Y., Comparative study of thiol-free amphiphilic hyperbranched and linear polymers for the stabilization of large gold nanoparticles in organic solvent, *J. Colloid. Interf. Sci.* 2009, **337**, 485–491.
- [80] Cho W. S., Cho M., Jeong J., Choi M., Han B. S., Shin H. S., Hong J., Chung B. H., Jeong J., Cho M. H., Size-dependent tissue kinetics of PEG-coated gold nanoparticles, *Toxicol. Appl. Pharm.*, **245**, (2010)116–123.
- [81] Zhang Z., Wang F., Chen F., Shi G., Preparation of polythiophene coated gold nanoparticles. *Mater. Lett.*, **60**, (2006)1039–1042.
- [82] Sun H., Dong S. Y., Feng J. L., Yin X. J., Zhao X. C., Enhanced sunlight photocatalytic performance of Sn-doped ZnO for methylene blue degradation, *J. Mol. Catal. A: Chem.* **335**(1-2), (2011)145-150.
- [83] Olteanu N. L., Meghea A., Enachescu M., Mihaly M., Tuning gold nanoparticles size and surface charge by oil-in-water microemulsion template, *Dig. J. Nanomater. Bios.*, **8**(4), (2013)1687 – 1697.
- [84] Lee C. H., Lin T. S., Lin H. P., Zhao Q., Liu S. B., Mou C. Y., *Microporous Mesoporous Mater.*, **57**, (2003)199.
- [85] Signorini R., Zerbetto M., Meneghetti M., Bozio R., Maggini M., De Faveri C., Prato M., Scorrano G., *Chem. Commun.* 1996, 1891.
- [86] Sariciftici N. S., Heeger A. J., *Proc. SPIE-Int. Soc. Opt. Eng.*, **76**, (1995)2530.
- [87] Kroto H. W., Heath J. R., O'Brien S. C., Curl R. F., Smalley R. E., *Nature*, **318**, (1985)162.
- [88] Tsoncheva T., Rosenholm J., Linden M., Kleitz F., Tiemann M., Ivanova L., Dimitrov M., Paneva D., Mitov I., Minchev C., Critical evaluation of the state of iron oxide nanoparticles on different mesoporous silicas prepared by an impregnation method, *Microporous Mesoporous Mat.* **112**(1-3), (2008)327-337.
- [89] Lizama L., Amezcua J. C., Klimova T., Development of new hybrid TiO<sub>2</sub>/SBA-15 mesoporous molecular sieves and their use as support for deep hydrodesulphurization NiMo catalyst, *Surf. Sci. Catal.*, **174**(2), (2008)1351-1354.
- [90] Boubekr F., Davidson A., Casale S., Massiani P., Ex-nitrate Co/SBA-15 catalyst prepared with calibrated silica grains: information given by TPR, TEM, SAXS and WAXS, *Microporous Mesoporous Mat.*, **141**(1-3), (2011)157-166.
- [91] Jun S., Ryoo R., Aluminum impregnation into mesoporous silica molecular sieves for catalytic application to Friedel-Crafts alkylation, *J. Catal.*, **195**(2), (2000)237-243.
- [92] Hu X., Foo M. L., Chuah G. K., Jaenicke S., Pore size engineering on MCM-41: selectivity tuning of heterogenized AlCl<sub>3</sub> for the synthesis of linear alkyl benzenes, *J. Catal.*, **195**(2), (2000)412-415.
- [93] Park S. K., Kurshev V., Luan Z., Lee C. W., Kevan L., Reaction of NO with copper ions in Cu(II) exchanged ZSM-5 zeolite: electron spin resonance, electron spin echo modulation and Fourier transform infrared spectroscopy, *Microporous Mesoporous Mat.*, **38**(2-3), (2000)255-266.

- [94] Ahn W. S., Lee D. H., Kim T. J., Kim J. H., Seo G., Ryoo R., Post synthetic preparation of titanium-containing mesopore molecular sieve, *Appl. Catal. A*, **181**(1), (1999)39-49.
- [95] Pirouzmand M., Amini M. M., Safari N., Immobilization of iron tetrasulfophthalocyanine on functionalized MCM-41 mesoporous silicas: catalysts for oxidation of styrene, *J. Coll. Interf. Sci.*, **319**(1), (2008)199-205.
- [96] Fechete I., Donnio B., Ersen O., Dintzer T., Djeddi A., Garin F., Single crystals of mesoporous tungstenosilicate V-MCM-48 molecular sieves for the conversion of methylcyclopentane (MCP), *Appl. Surf. Sci.*, **257**(7), (2011)2791-2800.
- [97] Anas K., Mohammed K. K. Y., Synthesis, characterization and hydrodesulphurisation activity of CoMo/ $\gamma$ -Al<sub>2</sub>O<sub>3</sub> catalyst prepared through molecular designed dispersion method, *Appl. Catal. A*, **264**(2), (2004)213-217.
- [98] Collart O., Van Der Voort P., Vansant E. F., Gustin E., Bouwen A., Schoemaker D., Ramachandra Rao R., Weckhuysen B. M., Schoonheydt R. A., Spectroscopic characterization of an MoO<sub>x</sub> layer on the surface of silica. An evaluation of the molecular designed dispersion method, *Phys. Chem. Chem. Phys.*, **1**(3), (1999)4099-4104.
- [99] Macwan D. P., Dave P., Chaturvedi S., A review of nano-TiO<sub>2</sub> sol-gel type synthesis and its application, *J. Mater. Sci.*, **46**(11), (2011)3669-3686.
- [100] Karami A., A Synthesis of TiO<sub>2</sub> nano-powder by the sol-gel method and its use as a photocatalyst, *J. Iran. Chem. Soc.*, **7**(7), (2010)S154-160.
- [101] Piccaluga G., Corrias A., Ennas G., Musinu A., Sol-Gel Preparation and Characterization of Metal and Metal-Oxide Silica Nanocomposites, *Mater. Sci. Foundations, Editura Trans. Tech. Publications, Uetikon*, 2000.
- [102] Andersson A., Hunderi O., Granqvist C.G., Nickel pigmented anodic aluminum oxide for selective absorption of solar energy, *J. Appl. Phys.*, **51**, (1980)754-764.
- [103] Kameya Y., Hanamura K., Enhancement of solar radiation absorption using nanoparticle suspension, *Sol. Energy*, **85**, (2011)299-307.
- [104] Hirsch L. R., Stafford R. J., Bankson J. A., Sershen S. R., Rivera B., Price R. E., Hazle J. D., Halas N. J., West J. L., Nano shell mediated near-infrared thermal therapy of tumors under magnetic resonance guidance, *Proceedings of the National Academy of Sciences of the United States of America*, **100**, (2003)13549-13554.
- [105] Chou C. S., Lin Y. J., Yang R. Y., Liu K. H., Preparation of TiO<sub>2</sub>/NiO composite particles and their applications in dye-sensitized solar cells, *Adv. Powder Technol.*, **22**, (2011)31-42.
- [106] Sebastian P. J., Quintana J., Avila F., Retention of the high optical absorptance in thermally aged black chrome on variably sensitized Cu, *Sol. Energy Mater. Sol. Cells*, **45**, (1997)65-74.
- [107] Nahar N. M., Mo G. H., Ignatiev A., Development of an Al<sub>2</sub>O<sub>3</sub>-Co Selective Absorber for Solar Collectors, *Thin Solid Films*, **172**, (1989)19-25.
- [108] Nuru Z. Y., Arendse C. J., Nemutudi R., Nemraoui O., Maaza M., Pt-Al<sub>2</sub>O<sub>3</sub> nanocoatings for high temperature concentrated solar thermal power applications, *Physica B*, **407**, (2012)1634-1637.
- [109] Stephen Sathiaraj T., Thangaraj R., AlSharbaty H., Agnihotri O. P., Optical properties of selectively absorbing R.F. sputtered Ni-Al<sub>2</sub>O<sub>3</sub> composite films, *Thin Solid Films*, **195**, (1991)33-42, Elsevier.
- [110] Zhang Q. C., Yin Y., Mills D. R., High efficiency Mo-Al<sub>2</sub>O<sub>3</sub> cermet selective surfaces for high-temperature application, *Sol. Energy Mater. Sol. Cells*, **40**, (1996)43-53.
- [111] Qi-Chu Zhanga, Shenb Y. G., High performance W-AlN cermet solar coatings designed by modelling calculations and deposited by DC magnetron sputtering, *Sol. Energy Mater. Sol. Cells*, **81**, (2004)25-37.
- [112] Maziere-Bezes D., Valignat J., Optical properties of gold-magnesia selective cermets, *Sol. Energy Mater.*, **7**, (1982)203-211.
- [113] Khamlich S., Nemraoui O., Mongwaketsi N., McCrindle R., Cingo N., Maaza M., Black Cr/a-Cr<sub>2</sub>O<sub>3</sub> nanoparticles based solar absorbers, *Physica B*, **407**, (2012)1509-1512.
- [114] Mandal S. K., Roy R. K., Pal A. K., Surface plasmon resonance in nanocrystalline silver particles embedded in SiO<sub>2</sub> matrix, *J. Physics D: Appl. Phys.*, **35**, (2002)2198-2205.

- [115] Henghua Deng, Dongfang Yang, Bo Chen, Chii-Wann Lin, Simulation of surface plasmon resonance of Au-WO<sub>3-x</sub> and Ag-WO<sub>3-x</sub> nanocomposite films, *Sens. Actuators, B*, **134**, (2008)502–509.
- [116] Camelio S., Toudert J., Babonneau D., Girardeau T., Tailoring of the optical properties of Ag:Si<sub>3</sub>N<sub>4</sub> nanocermet by changes of the cluster morphology, *Appl. Phys. B*, **80**, (2005)89–96.
- [117] Barshilia H. C., Prashant Kumar, Rajam K.S., Biswas A., Structure and optical properties of Ag-Al<sub>2</sub>O<sub>3</sub> nanocermet solar selective coatings prepared using unbalanced magnetron sputtering, *Solar Energy Materials and Solar Cells*, **95**, (2011)1707–1715.
- [118] Mihaly M., Rogozea E. A., Olteanu N. L., Petcu A. R., Lazar C. A., Meghea A., Tuning the colour of solar absorbers by changing chromophore nature and nanoparticle size, Sustainable Energy in the built Environment – steps towards nZEB, *Proceedings of the Conference for Sustainable Energy (CSE)*, (2014)311-325.
- [119] A. Duta, L. Isac, A. Milea, E. Ienei, D. Perniu, Coloured solar-thermal absorbers – a comparative analysis of cermet structures, *Energy Procedia*, **48**, (2014)543-553.
- [120] Das J., Yang H., *J. Phys. Chem., C* **113**, (2009)6093.
- [121] Zhang L.Y., Yuan R., Chai Y.Q., Li X.L., *Anal. Chim. Acta.*, **596**, (2007)99.
- [122] Yuan R., Tang D. P., Chai Y. Q., Zhong X., Liu Y., Dai J. Y., *Langmuir*, **20**, (2004)7240.
- [123] De La Escosura-Muñiz A., Sanchez-Espinel C., Diaz-Freitas B., Gonzales-Fernandez A., Maltez-Da Costa M., Merkoçi A., *Anal. Chem.*, **81**, (2009)10268.
- [124] Ambrosi A., Castaneda M. T., Killard A. J., Smyth M. R., Alegret S., Mercoci A., *Anal. Chem.*, **79**, (2007)5232.
- [125] De La Escosura-Muñiz, A., Maltez-Da Costa, M., Merkoçi, A., *Biosens. Bioelectron.*, **24**, (2009)2475.
- [126] Fleancu M., Mihaly M., Bojin D., Enachescu M., Anicai L., Study of Electrocatalytic Characteristics of Au Nanoparticles Prepared by Microemulsion Assisted Photoreduction Procedure, *Rev. Chim.*, **63**(12), (2012)1261-1265.
- [127] Rogozea E. A., Meghea A., Olteanu N. L., Bors A., Mihaly M., Fullerene-modified silica materials designed for highly efficient dyes photodegradation, *Mater. Lett.*, **151**, (2015)119–121
- [128] Sahraoui B., Pranaitis M., Iliopoulos K., Mihaly M., Comanescu A. F., Moldoveanu M., Rau I., Kaz'ukauskas V., Enhancement of linear and nonlinear optical properties of deoxy-ribonucleic acid-silica thin films doped with rhodamine, *Appl. Phys. Lett.*, **99**, (2011) 243304.